SOLUTE DISPERSION IN LIQUID-SOLID CHROMATOGRAPHIC COLUMNS

Thesis for the Degree of Ph. D.

MICHIGAN STATE UNIVERSITY

Martin C. Hawley

1964

This is to certify that the

thesis entitled

SOLUTE DISPERSION
IN LIQUID-SOLID CHROMATOGRAPHIC COLUMNS

presented by

Martin C. Hawley

has been accepted towards fulfillment
of the requirements for

Ph.D. degree in Chemical Engineering

M. H. Chetrick
Major professor

Date June 12, 1964

O-169

ABSTRACT

SOLUTE DISPERSION IN
LIQUID-SOLID CHROMATOGRAPHIC
COLUMNS

by Martin C. Hawley

Improvement of the scale-up procedure for liquid-solid chromatographic columns was the overall objective of this research. It was assumed that an axial dispersed, plug flow model with adsorption occurring would describe this unsteady state process. Theoretically, it was shown that the spread of a pulse of solute, as it passed between two measuring points, was the sum of the spreads of the adsorption and the dispersion process.

It was thought that the unreliability of the scale-up procedure was due to the liquid velocity effects and not dependent upon the adsorption process. Therefore, an experimental investigation of the operating variables in the absence of the adsorption was undertaken. The effects of the variables (column diameter and length, particle diameter, and pulse viscosity) were evaluated by their effect on the axial dispersion coefficient.

The pulse input method was utilized for the calculation of axial dispersion coefficients. These coefficients were evaluated from concentration versus time data of a tracer at two positions in a bed of glass spheres.

The solute was a dilute aqueous sodium chloride solution and the concentration-time data were obtained at two positions in the bed by

electrolytic conductance. The column diameter had no effect on the axial dispersion coefficient for interstitial velocities between 0.1 and 20 ft/hr and in this same velocity range. a high pulse viscosity did not affect the dispersion coefficient. It was also shown that the axial dispersion coefficient is proportional to the particle diameter, 0.0047 and 0.0071 inch diameter glass spheres. The average Peclet Number ($P_e = \frac{ud_p}{D}$) was 0.22 for modified Reynolds Numbers between 10^{-3} and 10^{-1}.

SOLUTE DISPERSION IN LIQUID-SOLID CHROMATOGRAPHIC COLUMNS

By

Martin C. Hawley

A THESIS

Submitted to
Michigan State University
in partial fulfillment of the requirements
for the degree of

DOCTOR OF PHILOSOPHY

Department of Chemical Engineering

1964

To Donna and Valerie

ACKNOWLEDGMENT

The author gratefully acknowledges the Upjohn Company and Consumers Power Company for financial support of this work.

Appreciation is extended to Dr. R. A. Zeleny and Dr. D. K. Anderson for their guidance during the course of the project. Appreciation is also extended to Mr. W. B. Clippinger for his help in the construction of the apparatus.

The understanding and patience of the author's wife, Donna, is sincerely appreciated.

TABLE OF CONTENTS

	Page
ABSTRACT	
ACKNOWLEDGMENT	i
TABLE OF CONTENTS	iii
LIST OF FIGURES	v
LIST OF TABLES	vi
INTRODUCTION	1
STATEMENT OF THE PROBLEM	4
Axial Dispersion With No Adsorption	15
Adsorption in the Bed with No Axial Dispersion	16
Infinitely Long Bed with Both Axial Dispersion and Adsorption	16
AXIAL DISPERSION IN PACKED BEDS	20
Diffusion Model	20
Solutions to the Diffusion Equation	25
The Mixing Cell Model	32
The Random-Walk Model	33
Comparison of Models	35
THE EXPERIMENTAL PROGRAM	39
Viscous Fingering	40
End Effects	41
Objectives	41
APPARATUS AND PROCEDURE	42
The Flow System	42
The Tracer	42

Packing Material 45

Conductance Cells 45

The Measuring Circuit 49

Packing Procedure 51

Run Procedure 51

Calculation of the Dispersion Coefficient from the Data 53

RESULTS AND DISCUSSION 56

Column Diameter 57

Pulse Viscosity 57

Particle Diameter 57

Column Length 61

Comparison With Other Work 61

CONCLUSIONS 66

APPENDIX I - Reynold's Method of Treating Turbulence or Eddies 67

APPENDIX II - Explanation of Pulse Skewness 69

APPENDIX III - The Solution to Equation (104) 72

NOMENCLATURE 80

BIBLIOGRAPHY 82

LIST OF FIGURES

		Page
1.	Diagram of the Adsorbing and Non-adsorbing Bed	4
2.	Increment of Bed	5
3.	Side-stepping Model of Dispersion	21
4.	Comparison of The Concentration Profiles of the Diffusion and Random-Walk Models	37
5.	Schematic of Flow Equipment	43
6.	Specific Conductance of Sodium Chloride at 25° C.	44
7.	Specific Conductance of Sucrose with a Trace Amount of NaCl at 25° C.	46
8.	Plexiglas Conductivity Cell for One-half Inch Column	47
9.	Six-Inch Conductivity Cell	48
10.	Electrical Circuit for Conductance Measurements	50
11.	Schematic of Rectifying Amplifying Circuit	52
12.	Conductance versus Time Plot of a Run	55
13.	D/D_v versus $4Mu/D_v$ for Column Diameter Comparison	58
14.	D versus u for Pulse Viscosity Comparison	59
15.	D versus u for Particle Diameter Comparison	60
16.	D/D_v versus $4Mu/D_v$ for Particle Diameter Comparison	62
17.	ud_p/D versus $4M\rho/\mu$ for Comparison With Other Work	63
18.	Plot of CV/Q versus $\frac{W}{V}t$ to Show Skewness	70

LIST OF TABLES

		Page
I.	Data for 1/2-inch column; .0071 inch glass beads; 3 cells equally spaced; 12 inches long	74
II.	Data for 1/2-inch column; .0071 inch glass beads; 2 cells 18 inches apart	75
III.	Data for 1/2-inch column; .0047 inch glass beads; 2 cells 18 inches apart	76
IV.	Data for 6-inch column; .0071 inch glass beads; 3 cells 6 and 12 inches apart	77
V.	Data for 6-inch column; .0071 inch glass beads; 2 cells 12 inches apart	78
VI.	Data for 100 Centipoise Sugar Solution with a Trace of NaCl as Pulse	79

INTRODUCTION

At the present time the scaling up of liquid-solid chromatographic columns is unreliable. A chromatographic separation may be accomplished in a small laboratory column, but when the process is scaled to industrial size, it does not always work as predicted by the laboratory model.

A liquid-solid chromatographic process is a separation technique which is effected in a packed bed. The separation is due to the difference in adsorptivities of the components being separated by the solid material. To visualize this unsteady state process, consider a bed packed with a solid which has an affinity for the components to be separated. For simplicity, the separation of two components will be considered. A solvent is continually flowing through the packed bed and at time zero the two components to be separated are introduced uniformly as a pulse across the top of the bed. As they move through the bed, these two components become separated from each other because they have different adsorptivities. The magnitude and the relative difference in the adsorptivities of the two components prescribes the length of bed which will effect the separation.

Chromatography is used primarily as an analytic tool in the laboratory, but in the pharmaceutical industry it is sometimes used as an industrial separation technique. The process is a batch type operation and normally low flow rates are used. It is not usually considered an economical means of separation, but the pharmaceutical industry, on the other hand, deals with valuable compounds, so when

other more conventional separating techniques fail, sometimes chromatography is used. Unfortunately, the nature of the components common to the pharmaceutical industry (their adsorptivities, diffusivities, etc.) is usually unknown. Since the properties of the components are unknown, one has to try various combinations of solvents and packings before a suitable combination is found. After a combination of solvent and packing material is found which will separate the components, the operating variables are analyzed in the laboratory. Therefore, the usual scale-up procedure is to first obtain the desired separation in a small laboratory sized column and then increase the size of the column according to the amount of material to be separated.

In order to keep the time required for the separation short and the pressure drop low, it is usually desirable to have the column as short as possible. In the laboratory the length of column is optimized with respect to the pressure drop and the time required for the separation. Theoretically, it is justifiable to increase the cross sectional area of the column in proportion to the amount of material to be separated without changing the length. In practice, this is the scale-up method along with increasing the length a certain amount only for good measure.

Since this method of scale-up does not always work, a fundamental approach to the scale-up problem will be given here, such that the scale-up procedure will be more reliable.

Chromatography can be thought of as being composed of two separate processes superimposed on each other. They are:

1. Fluid flowing in a packed bed
2. A sorption process.

It is proposed here that the unreliability in the current scale-up procedure is due to the fluid flow part of the process. Therefore, there must be a factor or a combination of factors which change with the column diameter, such that the separation achieved in columns of different diameters is not the same.

Theoretically, this investigation will show how the two processes, fluid flow and adsorption, can be separated. An experimental investigation of some factors which may change the flow characteristics with column diameter is also reported.

STATEMENT OF THE PROBLEM

Consider a packed bed with two concentration measuring devices, one at X_o the other at X_m (Figure 1).

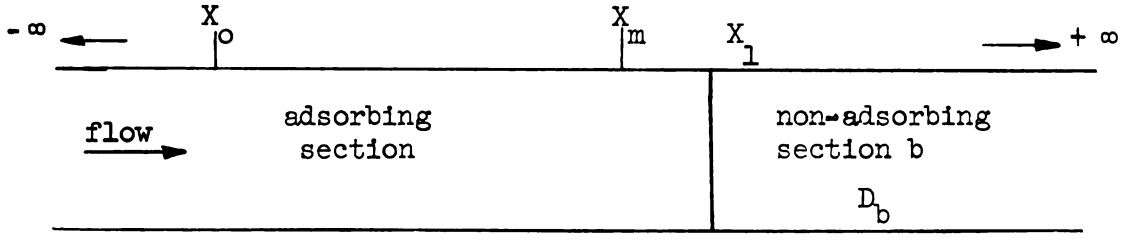

Figure 1. Diagram of the Adsorbing and Non-adsorbing Bed.

A shot of tracer is injected upstream from X_o into the bed in which a solvent is continually flowing with volumetric flow rate W. The surface of the packing has an affinity for the solute, hence unsteady state adsorption takes place inside the bed.

The bed is constructed with an adsorbing section followed by a non-adsorbing section. The two sections are further distinguished by different effective axial dispersion coefficients, D and D_b respectively.

Three assumptions made for this process are:

1. The tracer is injected uniformly across the cross section of the bed.
2. The flow is assumed uniform over the cross section of the bed; as a result radial diffusion can be neglected.
3. The adsorption isotherm is assumed to be linear.

This process may be characterized by two mass transport processes, convection and axial dispersion.

The concentration C_A is the average value for species A across a section of this column and the amount of transfer by dispersion is assumed to be proportional to the axial concentration gradient $\frac{\partial C_A}{\partial X}$. This is analogus to Fick's law for molecular diffusion. It is shown in Appendix I that the axial dispersion coefficient D is the sum of the molecular diffusivity and an eddy diffusivity.

A material balance of component A is made on an incremental length of packed bed as illustrated in Figure 2.

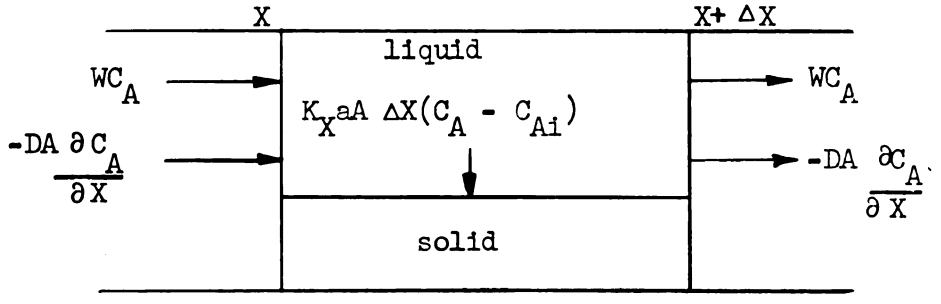

Figure 2. Increment of Bed.

The terms which describe the input and the output of material for each component are similar to those of component A. This tacitly assumes there are no interactions (i.e., component B does not affect the isotherm of A and so on).

The equations which describe the process of this system are

the equations of conservation of component A

(Liquid Phase)

$$\frac{\partial^2 C_A}{\partial X^2} - \frac{W}{D\epsilon A}\frac{\partial C_A}{\partial X} - \frac{K_x a}{D\epsilon}(C_A - C_{Ai}) = \frac{1}{D}\frac{\partial C_A}{\partial t} \quad \text{for } X \leq X_1 \tag{1}$$

$$\frac{\partial^2 C_A}{\partial X^2} - \frac{W}{D_b \epsilon_b A_b}\frac{\partial C_A}{\partial X} = \frac{1}{D_b}\frac{\partial C_A}{\partial t} \quad \text{for } X \geq X_1 \tag{2}$$

(Solid Phase)

$$\frac{K_x a}{1-\epsilon}(C_A - C_{Ai}) = \frac{\partial C_{As}}{\partial t} \quad \text{for } X \leq X_1 \tag{3}$$

$$C_{As} = 0 \quad \text{for } X \geq X_1 \tag{4}$$

assume that $C_{As} = mC_{Ai}$ (5)

where

- A = cross-sectional area of tube
- a = solids transfer area per volume
- C_A = concentration of species A in the liquid
- C_{Ai} = concentration of species A at the solid-liquid interface
- C_{As} = concentration of A on the solid
- D = axial dispersion coefficient
- ϵ = void fraction of bed
- K_x = mass transfer coefficient
- m = equilibrium constant defined by equation (5)
- t = time

W = volumetric flow rate

X = axial distance variable.

Equations (1) through (5) are solved by using the initial condition that $C_A = 0$ when $t = 0$ for $X \geq X_o$, along with the boundary conditions

$$\text{at} \quad X = X_o , \quad C_A = C_{Ao}(t) \qquad \text{for} \quad t \geq 0 . \tag{6}$$

$$\text{at} \quad X = X_1 , \quad C_A(X_1^-) = C_A(X_1^+) \tag{7}$$

$$\text{and} \quad C_A(X_1^-) - \frac{D\epsilon A}{W} \frac{\partial C_A}{\partial X}(X_1^-) = C_A(X_1^+) - \frac{D_b \epsilon_b A_b}{W} \frac{\partial C_A}{\partial X}(X_1^+) \tag{8}$$

$$\text{at} \quad X = \infty , \quad C_A(t, \infty) = \text{finite} \qquad \text{for} \quad t \geq 0 \tag{9}.$$

A restriction on $C_{AO}(t)$ is that it must be a "hump" function of time. This represents a pulse input. Aris[5] has given the mathematical restrictions for $C_{AO}(t)$. Boundary conditions (7) and (8) state that both the concentration and the flux are continuous at $X = X_1$.

The complete solution of equations (1) through (9) for C_A, C_{As}, and C_{Ai} in closed form, at the present time, is not possible, but by utilizing some formal mathematical properties of the Laplace transform it will be shown that it is not necessary to know the complete solution.

For convenience C_A, C_{Ai}, and C_{As} will be normalized such that

$$C = \frac{C_A}{\int_0^\infty C_A \, dt} \tag{10}$$

$$C_i = \frac{C_{Ai}}{\int_0^\infty C_A \, dt} \tag{11}$$

$$C_s = \frac{C_{As}}{\int_0^\infty C_A \, dt} \tag{12}$$

where

$$\int_0^\infty C_A \, dt = \frac{Q}{W} \tag{13}$$

and

Q = the total amount of A in the pulse

W = volumetric flow rate

Since $C = W C_A/Q$,

thus $$\int_0^\infty C \, dt = 1 \tag{14}.$$

Thus, the subscript A may be dropped from equations (1) through (9) and this set of boundary value equations is solved using the Laplace transform method. Since we are interested in that portion of the bed in which the adsorption process takes place, we will solve for the Laplace transform concentration $\overline{C}$ when $X \leq X_1$, that is the section of the bed containing both measuring points. If the Laplace transform of the concentration ($\overline{C}$) is known, then the nth moment of the concentration is defined by

$$B_n = (-1)^n \left[\frac{\partial^n \overline{C}}{\partial p^n}\right]_{p=0} \tag{15}$$

where p is the transform variable.

If all n moments of a distribution, in this case the concentration, are known, the distribution is completely described. Later, it will be shown that the mean and the variance, the first two moments of the concentration, give sufficient information to calculate the dispersion

coefficient from pulse input data. This is very important since higher moments become very laborious to calculate.

The Laplace transform of C with respect to t, $\bar{C}$, is

$$\bar{C} = \int_0^\infty \exp(-pt)\, C(t, x)\, dt \qquad (16).$$

Then, equation (5) is substituted into equation (3), and we take the Laplace transform of equation (1), (2), and (3).

The transformed equations are:

in the liquid phase

for $X \leq X_1$

$$\frac{\partial^2 \bar{C}}{\partial X^2} - \frac{W}{D\epsilon A}\frac{\partial \bar{C}}{\partial X} - \frac{K_x a}{D\epsilon}(\bar{C} - \bar{C}_i) = \frac{1}{D}\, p\, \bar{C} \qquad (1\text{-A})$$

for $X \geq X_1$

$$\frac{\partial^2 \bar{C}}{\partial X^2} - \frac{W}{D_b \epsilon_b A_b}\frac{\partial \bar{C}}{\partial X} = \frac{1}{D_b}\, p\, \bar{C} \qquad (2\text{-A})$$

and on the solid

for $X \leq X_1$

$$\frac{K_x a}{1-\epsilon}(\bar{C} - \bar{C}_i) = mp\bar{C}_i \qquad (3\text{-A})$$

for $X \geq X_1$

$$\bar{C}_s = 0 \qquad (4\text{-A}).$$

This set of equations now have been reduced from a set of partial differential equations in C to a set of ordinary differential equations in $\bar{C}$. $\bar{C}_i$ is substituted from equation (3) into equation (1) in terms of $\bar{C}$.

$$\frac{\partial^2 \bar{C}}{\partial X^2} - \frac{W}{D\epsilon A}\frac{\partial \bar{C}}{\partial X} - \frac{K_x a}{D\epsilon}\left[1 + \frac{\epsilon p}{K_x a} - \frac{1}{1 + \frac{mp(1-\epsilon)}{K_x a}}\right] \bar{C} = 0 \qquad (1\text{-B})$$

for $X \leq X_1$

$$\frac{\partial^2 \bar{C}}{\partial X^2} - \frac{W}{D_b \epsilon_b A_b}\frac{\partial \bar{C}}{\partial X} - \frac{p}{D_b}\bar{C} = 0 \qquad \text{for } X \geq X_1 \qquad (2\text{-B}).$$

The transformed boundary conditions are:

$$\text{at} \quad X = X_o, \qquad \bar{C} = \bar{C}_o(p) \qquad (6\text{-A})$$

$$\text{at} \quad X = X_1, \qquad \bar{C}(X_1^-) = \bar{C}(X_1^+) \qquad (7\text{-A})$$

and

$$\bar{C}(X_1^-) - \frac{D\epsilon A}{W}\frac{\partial \bar{C}}{\partial X}(X_1^-) = \bar{C}(X_1^+) - \frac{D_b \epsilon_b A_b}{W}\frac{\partial \bar{C}}{\partial X}(X_1^+) \qquad (8\text{-A})$$

and at $X = \infty$, $\bar{C}$ = finite (9-A).

Equations (1) and (2) are solved simultaneously with the transformed boundary conditions to obtain $\bar{C}$ for $X \leq X_1$.

$$\bar{C}(X, p) = \bar{C}_o(p)\ F(X, p) \qquad (17)$$

where, for $X \leq X_1$

$$F(X, p) = \frac{A \exp\left[\frac{s}{2} L\right]\left[G - H \exp\left[s\zeta\right]\right]}{G - H \exp\left[s(\zeta + L)\right]} \qquad (18)$$

$$A = \exp\left[\frac{b}{2} L\right]$$

$$L = X_m - X_o$$

$$\zeta = X_1 - X_m$$

$$b = \frac{W}{D\epsilon A}$$

$$s = \sqrt{b^2 + 4f}$$

$$f = e\left[1 - \frac{d}{p+d} + \frac{p}{De}\right]$$

$$d = \frac{mK_x a}{1-\epsilon}$$

$$e = \frac{K_x a}{D\epsilon}$$

$$G = R - \frac{b'}{b} s$$

$$R = \sqrt{b'^2 + 4\frac{p}{D_b}}$$

$$b' = \frac{W}{D_b \epsilon_b A_b}$$

$$H = R + \frac{b'}{b} s .$$

Expanding the functions $\bar{C}$, $\bar{C}_o$, and F in a Maclaurin series in powers of the Laplace transform variable p, there results:

$$\bar{C}(X, p) = \bar{C}(X, 0) + \sum_{n=1}^{\infty} \frac{1}{n!} \left[\frac{\partial^n \bar{C}}{\partial p^n}\right]_{p=0} p^n \tag{19}$$

$$\bar{C}_o(p) = \bar{C}_o(o) + \sum_{n=1}^{\infty} \frac{1}{n!} \left[\frac{\partial^n \bar{C}_o}{\partial p^n}\right]_{p=0} p^n \tag{20}$$

$$F(X, p) = F(X, 0) + \sum_{n=1}^{\infty} \frac{1}{n!} \left[\frac{\partial^n F}{\partial p^n}\right]_{p=0} p^n \tag{21}$$

From equation (16) it is readily seen that both $\bar{C}(X,o)$ and $\bar{C}_o(o)$ are equal to $\int_0^{\infty} C\, dt$ which is 1.

By substituting the expansions,(19), (20) and (21) into equation (17) and equating coefficients of p, it is easily shown that

$$F(X, 0) = 1 \tag{22}$$

$$\left[\frac{\partial F}{\partial p}\right]_{p=0} = \left[\frac{\partial \bar{C}}{\partial p}\right]_{p=0} - \left[\frac{\partial \bar{C}_o}{\partial p}\right]_{p=0} \tag{23}$$

and

$$\left[\frac{\partial^2 F}{\partial p^2}\right]_{p=0} - \left[\frac{\partial F}{\partial p}\right]^2_{p=0} = \left[\left[\frac{\partial^2 \bar{C}}{\partial p^2}\right]_{p=0} - \left[\frac{\partial \bar{C}}{\partial p}\right]^2_{p=0}\right] - \left[\left[\frac{\partial^2 \bar{C}_o}{\partial p^2}\right]_{p=0} - \left[\frac{\partial \bar{C}_o}{\partial p}\right]^2_{p=0}\right] \tag{24}.$$

The terms on the left hand side of equations (23) and (24) can be evaluated by differentiation of equation (18). The terms on the right hand side of equations (23) and (24) are related to well known properties of the concentration distribution at X_m and X_o.

The definition of the Laplace transform

$$\bar{C} = \int_0^\infty \exp(-pt)\, C\, dt$$

and the first and second derivatives of $\bar{C}$ as p equals zero will be considered.

The first derivative with p equal zero is

$$\left[\frac{\partial \bar{C}}{\partial p}\right]_{p=0} = -\int_0^\infty t\, C\, dt \tag{25}.$$

The integral is recognized as the mean time, μ_m, of the concentration at X_m.

Therefore,

$$\left[\frac{\partial \bar{C}}{\partial p}\right]_{p=0} = -\mu_m \tag{26}$$

and similarly for $\bar{C}_o$

$$\left[\frac{\partial \bar{C}_o}{\partial p}\right]_{p=0} = -\mu_o \tag{27}$$

where μ_o is the mean time of the concentration at X_o. Then equation (23) is rewritten

$$\left[\frac{\partial \bar{F}}{\partial p}\right]_{p=0} = -(\mu_m - \mu_o) \tag{28}.$$

The second derivative of $\bar{C}$ with p equal zero is

$$\left[\frac{\partial^2 \bar{C}}{\partial p^2}\right]_{p=0} = \int_0^\infty t^2 C \, dt \tag{29}$$

and

$$\left[\frac{\partial^2 \bar{C}}{\partial p^2}\right]_{p=0} - \left[\frac{\partial \bar{C}}{\partial p}\right]^2_{p=0} = \int_0^\infty t^2 C \, dt - \mu_m^2 \tag{30}.$$

Equation (30) is rewritten as

$$\left[\frac{\partial^2 \bar{C}}{\partial p^2}\right]_{p=0} - \left[\frac{\partial \bar{C}}{\partial p}\right]^2_{p=0} = \int_0^\infty (t - \mu_m)^2 C \, dt \tag{31}$$

and the integral is recognized as the second moment about the mean, or the time variance σ_m^2 at X_m,

$$\sigma_m^2 = \left[\frac{\partial^2 \bar{C}}{\partial p^2}\right]_{p=0} - \left[\frac{\partial \bar{C}}{\partial p}\right]^2_{p=0} \tag{32}.$$

Similarly for $\bar{C}_o$

$$\left[\frac{\partial^2 \bar{C}_o}{\partial p^2}\right]_{p=0} - \left[\frac{\partial \bar{C}_o}{\partial p}\right]_{p=0} = \int_0^\infty (t - \mu_o)^2 C \, dt \tag{33}$$

and

$$\sigma_o^2 = \left[\frac{\partial^2 \bar{C}_o}{\partial p^2}\right]_{p=0} - \left[\frac{\partial \bar{C}}{\partial p}\right]^2_{p=0} \tag{34}$$

where σ_o^2 is the time variance of the concentration at X_o.

With these definitions equation (24) is written

$$\left[\frac{\partial^2 F}{\partial p^2}\right]_{p=0} - \left[\frac{\partial F}{\partial p}\right]^2_{p=0} = \sigma_m^2 - \sigma_o^2 \qquad (35).$$

Thus, from experimental data of concentration versus time at two positions in a bed, one can calculated $\mu_m - \mu_o$ and $\sigma_m^2 - \sigma_o^2$ as numbers. From this data the unknown parameters of the bed can be evaluated by equating these numbers to the respective equation, either (28) or (35). Differentiating equation (18) with respect to the transform variable p, we obtain,

$$\mu_m - \mu_o = \frac{L}{b}\left(\frac{e}{d} + \frac{1}{D}\right)$$

$$- \left[\frac{1}{D_b\, b'^2} - \left(\frac{e}{d} + \frac{1}{D}\right)\frac{1}{b^2}\right] \exp(-b\zeta)[\exp(-bL) - 1] \qquad (36).$$

The second derivative, minus the square of the first derivative, is

$$\sigma_m^2 - \sigma_o^2 = 2L\left[\frac{2}{d^2 b} + \frac{1}{b^3}\left(\frac{e}{d} + \frac{1}{D}\right)^2\right]$$

$$+ 4\left[\frac{1}{b^4}\left(\frac{e}{d} + \frac{1}{D}\right)^2 - \frac{1}{D_b^2\, b'^4} + \frac{1}{2}\,\frac{e}{b^2 d^2}\right][\exp(-bL) - 1]\exp(-b\zeta)$$

$$- 4(\zeta + L)\left[\frac{\left(\frac{e}{d} + \frac{1}{D}\right)}{b'^2\, b\, D_b} - \frac{1}{b^3}\left(\frac{e}{d} + \frac{1}{D}\right)^2\right]\exp[-b(L + \zeta)]$$

$$+ 4\zeta\left[\frac{\left(\frac{e}{d} + \frac{1}{D}\right)}{b'^2\, b\, D_b} - \frac{1}{b^3}\left(\frac{e}{d} + \frac{1}{D}\right)^2\right]\exp[-b\zeta]$$

$$+ \left[\frac{1}{D_b b'^2} - \frac{1}{b^2}\left(\frac{e}{d} + \frac{1}{D}\right)\right]^2 [\exp(-2bL) - 1]\exp(-2b\zeta) \qquad (37).$$

These are the desired but cumbersome results. There are three limiting cases for which the solutions to this problem are of interest. The results for $\mu_m - \mu_o$ and $\sigma_m^2 - \sigma_o^2$ will be tested for these limiting cases.

a). Axial Dispersion with No Adsorption

$$\frac{e}{d} = 0$$

and

$$\frac{e}{d^2} = 0$$

Let $bL = P$ and

$$\beta = \frac{b^2 D}{b'^2 D_b}$$

equation (36) becomes

$$\mu_m - \mu_o = \frac{\epsilon AL}{W} \left[1 - \frac{(\beta - 1)}{P}\right] [\exp(-p) - 1] \exp \frac{(-P\zeta)}{L} \qquad (38).$$

This is the difference of mean times which Bischoff[8] obtained for no adsorption. With the same values inserted into equation (37), the difference of variances is obtained.

$$\sigma_m^2 - \sigma_o^2 = \left(\frac{\epsilon AL}{W}\right)^2 \left[\frac{2}{P} + \frac{4}{P^2}(1 - \beta^2)(\exp(-P) - 1) \exp \frac{(-P\zeta)}{L}\right.$$

$$- \frac{4(\zeta + L)}{PL}(\beta - 1) \exp\left(\frac{-P}{L}(\zeta + L)\right) + \frac{4\zeta}{PL}(\beta - 1) \exp \frac{(-P\zeta)}{L}$$

$$\left. + \frac{1}{P^2}(\beta - 1)^2 (\exp(-2P) - 1) \exp \frac{(-2P\zeta)}{L}\right] \qquad (39).$$

This equation also checks with the result of Bischoff.

As the bed goes to infinity, i.e. $\zeta \longrightarrow \infty$

$$(\mu_m - \mu_o)_\infty \longrightarrow \frac{\epsilon AL}{W} \tag{40}$$

$$(\sigma_m^2 - \sigma_o^2)_\infty \longrightarrow \left(\frac{\epsilon AL}{W}\right)^2 \frac{2}{P} \tag{41}.$$

b). Adsorption in the bed with no axial dispersion

For the case of adsorption, with no axial dispersion

$D = 0$

$b = \infty$

$$\frac{e}{db} = \frac{A}{W} \frac{(1-\epsilon)}{m}$$

$$\frac{1}{bD} = \frac{\epsilon A}{W} .$$

With these substitutions equation (36) reduces to

$$\mu_m - \mu_o = \frac{L A}{W m} [1 + \epsilon(m-1)] \tag{42}.$$

By inserting $D = 0$ into equation (37), it is seen that all the exponential terms go to zero because b goes to infinity. Also the $\frac{1}{b^3}\left(\frac{e}{d} + \frac{1}{D}\right)^2$ term is zero when $D = 0$. Therefore, only the first term for $\sigma_m^2 - \sigma_o^2$ remains:

$$\sigma_m^2 - \sigma_o^2 = \frac{2 L A}{W m^2} \frac{(1 - \epsilon)^2}{K_X a} \tag{43}.$$

c). Infinitely long bed with both axial dispersion and adsorption

For an infinite bed, $\zeta = \infty$ is inserted into equations (36) and (37), they reduce to

$$(\mu_m - \mu_o)_\infty = \frac{\epsilon AL}{W} + \frac{(1 - \epsilon) A L}{m W} \tag{44}$$

and the exponential terms in equation (37) are zero, hence

$$(\sigma_m^2 - \sigma_o^2)_\infty = \frac{2AL}{m^2 K_X a} \frac{(1-\epsilon)^2}{W} + \frac{2L}{W^3} (D\epsilon A)^3 \left[\frac{(1-\epsilon)}{\epsilon m D} + \frac{1}{D}\right]^2 \quad (45).$$

Let

$$\psi = \frac{(\sigma_m^2 - \sigma_o^2)_\infty}{(\mu_m - \mu_o)_\infty^2} \quad (46)$$

where ψ is a measure of the total spread of a pulse.

Then let

$$\psi_D = \frac{(\sigma_m^2 - \sigma_o^2)_\infty}{(\mu_m - \mu_o)_\infty^2} \quad (47)$$

$$\psi_A = \frac{(\sigma_m^2 - \sigma_o^2)_\infty}{(\mu_m - \mu_o)_\infty^2} \quad (48)$$

where ψ_D is the spread due to axial dispersion for an infinite tube, evaluated in case (a), and ψ_A is the spread due to adsorption, evaluated in case (b).

An interesting result of this case (c), is

$$\psi = \frac{2\,D\epsilon A}{WL} + \frac{2\,W}{ALK_X a} \left[\frac{1-\epsilon}{1+\epsilon(m-1)}\right]^2 \quad (49).$$

If we examine (a) for the infinite case we find that

$$\psi_D = \frac{2\epsilon AD}{WL} \quad (50)$$

and if we examine (b) for an infinite bed we find that

$$\psi_A = \frac{2\,W}{AL\,K_X a} \left[\frac{1-\epsilon}{1+\epsilon(m-1)}\right]^2 \quad (51).$$

Therefore, for the infinite tube case with both processes, the total spread of a pulse input is the sum of the axial dispersion and adsorption spreads. Therefore, we may write

$$\psi = \psi_D + \psi_A \qquad (52).$$

Van Deemter, Zuiderweg, and Klinkenberg[45] have shown that, if the concentration-time distribution were Gaussian, the dimensionless variance at a position in the bed is the sum of the dimensionless variances due to axial dispersion and adsorption. In this work, it has been shown that the difference in dimensionless variances between two planes in an infinitely long bed is the sum of the differences of dimensionless variances due to the axial dispersion and adsorption for any hump like input. That is, the restriction of a Gaussian distribution is removed.

There is a great experimental advantage in removing this restriction since it is impossible to introduce a perfect pulse input. Previous work[16,20] has required that the concentration time curve also be Gaussian at the measuring point. It is shown in Appendix II that any pulse input approaches a Gaussian time distribution for long columns. All previous investigators have made this a criterion for the design of their apparatus. Thus, both a long column and a perfect injection system were needed. The present work allows one to analyze data from short columns with no particular care taken to introduce the pulse into the column. The only requirement of the pulse is that it be "hump-like".

In summary, the relationship between the difference in variances and means between two points in a finite packed bed and the parameters of the bed is derived with both axial dispersion and adsorption occurring simultaneously. Three specific cases of this general solution are obtained and case (a) is compared with a previously derived result, first by Aris[2] and later, corrected by Bischoff[8].

In summary these three specific cases are:

(a) axial dispersion with uniform flow in both portions of the bed.

(b) adsorption process occurring in the first section of the bed with axial dispersion in the second section along with uniform flow.

(c) infinitely long bed with both adsorption and axial dispersion occurring simultaneously and individually with uniform flow.

As a result of considering case (c) the term

$$\psi = \frac{\sigma_m^2 - \sigma_o^2}{(\mu_m - \mu_o)^2}_{\infty}$$

from axial dispersion may be added to the corresponding term for adsorption to obtain the result for both processes occurring simultaneously. This is the mathematical justification for separating the two phenomena, axial dispersion and adsorption.

AXIAL DISPERSION IN PACKED BEDS

This discussion will present background material concerning dispersion, primarily in packed beds.

The three common approaches to dispersion are: (A) the diffusion model; (B) the mixing cell model; and, (C) the statistical approach. All three of these models have been analyzed theoretically and experimentally by many investigators.

Diffusion Model

The most widely used model for axial dispersion is the diffusion model, which assumes that the equations which apply to mass transfer of species are of the same form as those describing a molecular diffusion process.

The conservation equation is

$$D \frac{\partial^2 C}{\partial X^2} - u \frac{\partial C}{\partial X} = \frac{\partial C}{\partial t} \qquad (53).$$

It is shown in Appendix I that D, the dispersion coefficient, is the sum of the molecular and eddy diffusivities.

The use of the Fick's law equation for turbulent transfer has been discussed by Prausnitz[35]. He considers an observer traveling with the mean flow velocity, U_o.

Two packets of fluid, A and B of Figure 3, interchange by the following mechanism:

1. Fluid element A, coordinate (r_o, X-1) and traveling at U_o, encounters a solid particle and, in order to pass it, side-steps to position r_1, where its velocity is changed to U_1.

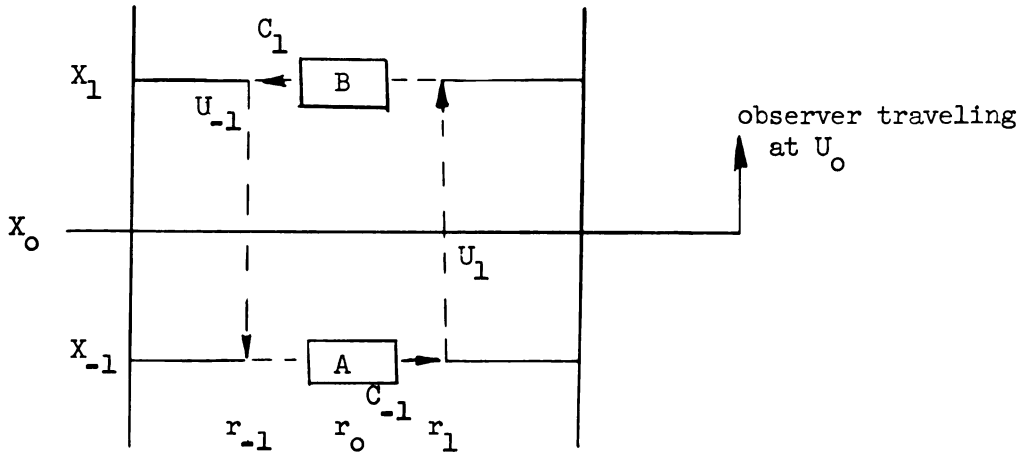

Figure 3. Side-stepping Model of Dispersion.

2. Fluid element B, coordinate (r_o, X_1) and traveling at U_o, encounters a solid particle and, in order to pass it, side-steps to position r_{-1} with a new velocity U_{-1}.

In order that A and B interchange positions in the stream, $(U_1 - U_o) = (U_o - U_{-1})$. The flowing fluid is a solution of a solute concentration C_1 at X_1 and C_{-1} at X_{-1}. Thus, there is a net flux of solute across the plane which is moving at velocity U_o and is given by:

$$\text{NET FLUX} = (U_1 - U_o)\, C_{-1} + (U_{-1} - U_o)\, C_1 \qquad (54).$$

The velocity increments in excess of U_o within a pore are given by

$$\frac{U_1 - U_o}{l_r} = -\frac{(U_{-1} - U_o)}{l_r} = \frac{\partial U}{\partial r} \qquad (55)$$

where l_r is the radial scale of mixing similar to the Prandtl mixing length for turbulent flow. It represents an average side stepping

distance. Similarily,

$$\frac{C_1 - C_{-1}}{l_X} = \frac{\partial C}{\partial X} \tag{56}$$

where l_X is the axial scale of mixing.

By inserting equations (55) and (56) back into equation (53), the net flux is given by:

$$\text{Net Flux} = - l_X l_r \frac{\partial U}{\partial r} \frac{\partial C}{\partial X} \tag{57}.$$

This simplified model shows how one can deduce an expression for the net flux in terms of the axial concentration gradient, the radial velocity gradient, and the axial and radial side-stepping lengths. By comparison with Fick's law for molecular diffusion the mixing or eddy diffusivity, D_e, is given by:

$$D_e = l_X l_r \frac{\partial U}{\partial r} \tag{58}$$

and the net flux due to mixing is

$$\text{Net Flux} = - D_e \frac{\partial C}{\partial X} \tag{59}.$$

This development justifies the use of a Fick's law diffusion model to describe eddy mass transfer. However, it is emphasized that the eddy diffusivity depends upon the flow characteristics of the flow region; whereas, the molecular diffusivity depends on the intrinsic properties of the fluid.

Prausnitz and Wilhelm[36] have obtained concentration fluctuations at high interstitial velocities which indicate orders of magnitudes and approximate values for the parameters in the eddy diffusivity. These

approximate values are $l_r = 1/4\ d_p$ where d_p is the particle diameter and $l_x = 7\ l_r$. From dimensional considerations a reasonable estimate for the order of magnitude of dU/dr is U/d_p.

Thus the value of the Peclet Number ($P_e = \frac{U\ dp}{D_e}$) is approximately two. This agrees, probably fortuitously, with experimental data, at turbulent flow conditions.

With this type of model one can predict qualitatively the effect of void fraction on the eddy diffusivity. As a first approximation the tendency for l_r to increase with void fraction will be compensated for by a tendency for dU/dr to decrease; however, l_x would be expected to increase. Thus one would expect an increase in the eddy diffusivity and a decrease in the Peclet Number with an increase of void fraction. This has been experimentally verified by Jacques[25]. The effect of particle diameter is similarly analyzed, and it is expected that the eddy diffusivity would increase proportionally with the particle diameter and as a result one would expect no change in the Peclet Number. This has been experimentally verified by Ebach and White[20].

The theory previously discussed is a generalization of the model proposed by Taylor[42] for flow in pipes. Taylor derived an equation to describe axial dispersion for turbulent flow in pipes.

$$D_e = 3.7\ d_t\ u\ \sqrt{\gamma} \qquad (60)$$

where

d_t = diameter of the pipe

u = mean flow velocity

and

γ is defined by

$$\tau_o = \frac{1}{2} \gamma \rho u^2 \tag{61}$$

where

τ_o = shear stress at wall of pipe

ρ = the density of the fluid.

γ is interpreted as a resistance coefficient for the flowing fluid.

In another paper, Taylor[43] derived the expression for the axial dispersion coefficient for laminar flow in a tube

$$D_{axial} = \frac{d_t^2 u^2}{192 D_v} \tag{62}$$

where D_v is the molecular diffusivity of the solute. Taylor's development shows that the dispersion is due to radial gradients.

Fluid flowing slowly in a packed bed will have dispersion characteristics which are a combination of the characteristics of a fluid flowing in a tube in both laminar and turbulent flow. If the fluid is actually in laminar flow in the interstices of a packed bed, it should exhibit turbulent-like dispersion characteristics, since the packing restricts the flow such that a laminar profile is not set up in the bed. The interstices are interconnected such that the boundary conditions and geometry of each cannot be represented mathematically as simply as those of a tube. Therefore, it is realistic to qualitatively describe dispersion in a packed bed of a slow moving fluid by the side-stepping model developed by Prausnitz[37].

Solutions to the Diffusion Equation

There are four types of boundary conditions which have been applied to equation (53) for dispersion in packed beds from which a description of the concentration profile is obtained. From these solutions and appropriate experimental data, one may obtain the value of the axial dispersion coefficient D. Three of these sets of conditions are for the unsteady state and the other is for the steady state.

The pulse input - This method is an unsteady state case of equation (53) solved with the following boundary conditions:

$$\text{at } t = 0, \quad C = 0 \quad \text{for } X > 0 \tag{63}$$

$$\text{at } X = \infty, \quad C = \text{finite} \quad \text{for} \quad t > 0 \tag{64}$$

and at $X = 0$ there is an infinitely high pulse of zero thickness introduced. The solution is approximately (Appendix III)

$$C(X, t) = \frac{Q}{V\sqrt{4\pi\ D/uX}} \exp\left[\frac{-(1 - \frac{ut}{X})^2}{\frac{4D}{uX}}\right] \tag{65}$$

where

$$Q = W \int_0^\infty C\, dt \tag{66}$$

which is the total solute injected.

The maximum value of C appears at

$$t_m = \frac{-D}{U^2} + \frac{D}{U^2}\left[1 + \left(\frac{XU}{D}\right)^2\right]^{1/2} \tag{67}$$

and can be approximated by

$$t_m = \frac{X}{U} - \frac{D}{U^2} \quad \text{when} \quad \left(\frac{XU}{D}\right)^2 >> 1 \tag{68}.$$

Equation (65) is in the form of a normal distribution with the variance given by

$$\sigma^2 = \frac{2D}{uL} \tag{69}.$$

The variance of the concentration-time distribution at X = L is determined experimentally, and D is calculated from equation (69).

The step input - Equation (53) is solved for a finite bed of length L with the following conditions:

$$\text{at } X = L \quad \frac{\partial C}{\partial X} = 0 \quad \text{for } t > 0 \tag{70}$$

and at X = 0 and t > 0

$$UC - D\frac{\partial C}{\partial X} = U C_o \tag{71}$$

where C_o is the concentration of the input, and at t = 0

$$C = 0 \qquad \text{for } X > 0 \tag{72}.$$

The set of equations to be solved in dimensionless form is

$$\frac{\partial C^*}{\partial \theta} + \frac{\partial C^*}{\partial y} = \frac{1}{4P'}\frac{\partial^2 C^*}{\partial y^2} \tag{73}$$

$$4P' C^* - \frac{\partial C^*}{\partial y} = 0 \quad \text{at } y = 0 \quad \text{for } \theta > 0 \tag{74}$$

$$\frac{\partial C^*}{\partial y} = 0 \quad \text{at } y = 1 \quad \text{for } \theta > 0 \tag{75}$$

$$C^* = 1 \quad \text{at} \quad \theta = 0 \quad \text{for } 0 < y < 1 \tag{76}$$

where

$$P' = \frac{UL}{4D} \qquad y = \frac{X}{L}$$

$$C^* = \frac{C_o - C}{C_o} \qquad \theta = \frac{U t}{L}$$

Brenner[12] has shown that the substitution of

$$C^*(y,\theta) = T(y,\theta)\exp(2P'y - P'\theta) \tag{77}$$

reduces equation (73) to the one dimensional head conduction problem

$$\frac{\partial T}{\partial \theta} = \frac{1}{\partial P'}\quad\frac{\partial^2 T}{\partial y^2} \tag{78}$$

with conditions

$$\frac{\partial T}{\partial y} - 2P'T = 0 \quad \text{at } y = 0 \text{ for } \theta > 0 \tag{79}$$

$$\frac{\partial T}{\partial y} + 2P'T = 0 \quad \text{at } y = 1 \text{ for } \theta > 0 \tag{80}$$

$$T(y,0) = \exp(-2P'y) \quad \text{at } \theta = 0 \tag{81}.$$

These boundary conditions correspond to convection from the ends of a slab into a media at zero temperature. Carslaw and Jaeger[17] have given the general solution of this arbitrary initial condition.

The solution to these equations is

$$C^*(y,\theta) = 2\exp[P(2y - \theta)] \times \sum_{K=1}^{\infty} P'\tau_K/(\tau_K^2 + P'^2 + P')$$

$$(\tau_K^2 + P'^2) \times [\tau_K \cos(2\tau_K y) + P' \sin(2\tau_K y)] \times \exp(-\tau_K^2\,\theta/P') \tag{82}$$

where the $\tau_K (K=1, 2..)$ are the positive roots, taken in order of increasing magnitude, of the transcendental equation

$$\text{Tan } 2\tau = \frac{2\tau P'}{\tau^2 - P'^2}, \quad \text{and } \tau \neq 0 \tag{83}.$$

Equation (82) converges too slowly to be of much use when P' is large and/or t is small. Brenner[12] developed an asymptotic solution by the Laplace transformation and has tabulated values of C* as a function of t for large values of P'. These can be used to calculate P' from experimental data, C-t for a given column.

The step input is also solved for an infinite column extending from $-\infty$ to $+\infty$. Initially, the section from $X = -\infty$ to $X = 0$ is filled with solute of concentration $C = C_o$, and for X greater than 0, $C = 0$. Thus the boundary conditions are:

$$\text{at } X = 0, \quad C = C_o \quad \text{for } t > 0 \tag{84}$$

$$\text{at } X = \infty, \quad C = 0 \quad \text{for } t > 0 \tag{85}$$

and at

$$t = 0, \quad \begin{cases} C = C_0 & \text{for } X < 0 \\ C = 0 & \text{for } X > 0 \end{cases} \tag{86}.$$

The solution to equation (53) with these conditions is given by Danckwerts[19]

$$\frac{C}{C_o} = \frac{1}{2}\left[1 - \operatorname{erf}\frac{(X - ut)}{(4\,Dt)^{1/2}}\right] \tag{87}$$

where

$$\operatorname{erf}(Z) = \frac{2}{\sqrt{\pi}} \int_0^Z \exp(y^2)\, dy \tag{88}.$$

By setting $X = L$ and differentiating equation (86) with respect to ut/L and evaluating when $ut = L$, one obtains

$$\left[\frac{\partial\left(\frac{C}{C_o}\right)}{\partial\left(\frac{ut}{L}\right)}\right]_{\frac{ut}{L}=1} = \frac{1}{2}\sqrt{uL/\pi D} \tag{89}.$$

From data of C/C_o versus ut/L, the slope at ut/L = 1 gives the value of D.

Frequency response technique - This is a quasi-steady state method for determining the parameters of the bed in which the solute concentration input to the bed is a sinusoidal function of time. The amplitude and the phase angle lag at the output section of the bed are related to the bed parameters.

The boundary conditions are represented by:

$$C = C_m + A\,(X, 0) \cos(\omega t) \qquad \text{at } X = 0 \qquad (90)$$

$$C = C_m \quad \text{or} \quad A = 0 \qquad \text{at } X = \infty \qquad (91).$$

Ebach and White[20] have shown the solution to equation (53) with these conditons is:

$$C\,(X, t) = C_m + A(0) \exp(-B) \cos(\omega t - \phi) \qquad (92)$$

where

$$B = -\frac{X u}{2 D}\left[1 - (\sqrt{1/4 + (2D\omega/u^2)^2} + 1/2)^{1/2}\right] \qquad (93)$$

and

$$\phi = \frac{X u}{2D}\left[\sqrt{1/r + (2D\omega/u^2)^2} - 1/2\right]^{1/2} \qquad (94)$$

and

A(o) = input amplitude

C_m = mean composition about which concentration oscillates

ω = angular frequency of periodic wave, rad/sec.

B and ϕ represent the decrease in amplitude and the phase shift of the output wave, respectively.

The ratio of the inlet amplitude to the outlet amplitude is given by

$$A_i/A_e = B \tag{95}.$$

Equation (93) is compared with (95) for experimental data and D is then calculated.

Steady state solution - Equation (53) is solved with the boundary conditions:

$$C = C_o \quad \text{at} \quad X = L \tag{96}$$

and

$$u\,C = D\,\frac{\partial C}{\partial X} \quad \text{at} \quad X = 0 \tag{97}.$$

Since the steady state is assumed

$$dC/dt = 0 \tag{98}$$

and the solution to this set of conditions is

$$C = C_o \exp\left[\frac{u}{D}(X - L)\right] \tag{99}.$$

These conditions correspond to a tracer being continuously injected downstream from the inlet of the column and the solution is for the concentration profile between the inlet to the bed and the tracer injection.

A plot of ln C versus X yields a slope of u/D from which D can be determined.

The four solutions to the diffusion equation (the pulse input, the step input, the frequency response technique, and the steady

state method) all represent different experimental techniques to calculate the axial dispersion coefficient D of equation (53). These solutions differ only in the boundary conditions which are applied. Consequently, D should have the same value under the same bed conditions for each technique.

The pulse input as given here requires the pulse to be of zero thickness and of infinite height. This is experimentally impossible, and in order to approximate this type of input, considerable care must be taken in the design of the injection system.

The method derived by Aris[2] and later corrected by Bischoff[8] (see Case (a) in Statement of Problem), allows one to calculate the axial dispersion coefficient with a minimum of assumptions. The only restrictions on the input are those given by Aris[5] which essentially state that the pulse input be a "hump like" function of time. This method requires two points of measurement rather than one. However, the column does not have to be long as in the case of the approximation of a normal distribution.

The step input method is a popular method of analysis and requires concentration versus time measurements at one position in the column, however, it is experimentally difficult to obtain a sharp step input.

The frequency response technique is probably the most difficult method experimentally. It takes a great deal of elaborate equipment to generate a sinusoidal concentration input. In addition, a fast response measuring technique is required.

The steady state method, in principle, is the simplest method for the determination of the axial dispersion coefficient.

However, u/D must have an order of magnitude of about 10 ft^{-1} to be practical. This is considerably smaller than the approximate value of 200 ft^{-1} for this work.

The Mixing Cell Model. The mixing cell model was first discussed by Kramers and Alberda[30] and later by other investigators.[6,15,16,35] They assumed the voids between the particles of packing may be considered as cells of complete mixing.

Equations (100, (101), and (102) describe a series of cells numbered from 0 to N, with the zeroth cell being fed a solution of concentration $C_f(t)$. It is assumed that the cells are initially free of solute, and their volumes and the flow rate are V and W, respectively.

$$W C_{N-1} - W C_N = V \frac{dC_N}{dt} \tag{100}$$

$$C_N = 0 \quad \text{at} \quad = 0 \tag{101}$$

$$W C_f - W C_o = V \frac{dC_o}{dt} \quad \text{for } t > 0 \tag{102}.$$

Aris and Amundson[6] have applied the Laplace transformation to equations (100), (101), and (102) and found $\bar{C}_N$, the Laplace transform of C_N,

$$\bar{C}_N = \left[\frac{W}{V}\right]^{N+1} \frac{\bar{C}_f}{(P + W/V)^{N+1}} \tag{103}$$

where p is the transform variable.

The inverse transform by means of the convolution integral is

$$C_N = \frac{1}{N!} \left[\frac{W}{V}\right]^{N+1} \int_0^t C_f(s)\,(t-s)^N \exp\left[-\frac{W}{V}(t-s)\right] ds \qquad (104)$$

which gives the concentration at the Nth mixing cell as a function of t and the input $C_f(s)$.

For a delta pulse function input, equation (104) has been integrated (see Appendix III) with the result

$$\frac{W\,C_N}{Q} = \frac{\left[\frac{W}{V}\,t\right]^{N+1}}{N!\;t} \exp\left(-\frac{W}{V}\,t\right) \qquad (105)$$

where Q is the amount of material injected.

Equation (105) is a relationship for the concentration of the Nth cell as a function of time for a pulse input.

For a step-function feed of tracer of concentration C_i at the inlet to a sequence of mixing cells, the concentration at cell N is given as a function time by:

$$\frac{C}{C_i} = 1 - \left[\frac{\left[\frac{W}{V}\,t\right]^N}{N!} + \frac{\left[\frac{W}{V}\,t\right]^{N-1}}{(N-1)!} + \ldots + 1\right] \exp\left(-\frac{W}{V}\,t\right) \qquad (106).$$

The Random-Walk Model. Jacques and Vermeulen[25] have developed a random-walk model for the transport of a tracer molecule through a packed bed. The random-walk of a tracer molecule through a packed bed is characterized by the advancement of the molecule from point to point in a some what erratic way, always moving in the direction of flow. The path followed by the molecule is made up of a succession of random steps involving different distances and occurring at different times.

Scheidegger[40] has pointed out that the fluid flow through porous media is governed by the Navier-Stoke's equations. It is the randomness of the media itself which leads to a stochastic treatment of the flow. The stochastic approach to the problem is based on the "ergodic hypothesis" which states the motion of a particle at any point in the media is independent of the particles at other points in the media.

Jacques and Vermeulen have derived a normalized probability density function $P_T(N)$ for this case such that

$$P_T(N)\, dT = \exp[-(N+T)]\, I_o(2\sqrt{NT})\, dT \qquad (107)$$

where

$N = L/h$ (number of steps) dimensionless length

$T = ut/h$ dimensionless time

and

L = length of bed

h = average length of steps

u = a characteristic velocity

t = time.

I_o is the zero-order Bessel function of the first kind with an imaginary argument.

$P_T(N)\, dT$ is the probability of finding a packet of fluid N mixing lengths from the inlet between time T and T + dT.

For a step function input of concentration C_o the equation for the concentration at plane N is

$$\frac{C}{C_o} = \int_0^T \exp[-(N+T)]\, I_o(2\sqrt{NT})\, dT \qquad (108).$$

Hennico, Jacques and Vermeulen[23] have tabulated values of C/C_o versus T for a step input for values of the parameter N. Their values are based on an approximation of equation (108) which is suggested by Klinkenberg[28].

The Klinkenberg approximation simplified equation (108) to

$$\frac{C}{C_o} = \frac{1}{2}\left[1 + \text{erf}\left[\sqrt{(N+1)\,\theta - 1/4} - \sqrt{N + 1/4}\right]\right] \quad (109)$$

where

$$\theta = \frac{T}{N+1} \quad .$$

For a pulse input of amount Q and a column having a void volume of V the concentration C is given by:

$$\frac{CV}{Q} = \exp\left[-(N+T)\right] I_o\left(Z\sqrt{NT}\right) \quad (110).$$

Comparison of Models. Several investigators[6,30,35] have shown that the cell size in the mixing-cell model corresponds to twice the mixing length in the diffusion model. The diffusion equation is

$$D\frac{\partial^2 C}{\partial X^2} - u\frac{\partial C}{\partial X} = \frac{\partial C}{\partial t} \quad (111).$$

The finite-difference form of the diffusion equation is

$$D\frac{\left[C_{x+\Delta x} - 2C_x + C_{x-\Delta x}\right]}{\Delta X^2} - \frac{u}{2}\frac{\left[C_{x+\Delta x} - C_{x-\Delta x}\right]}{\Delta X} = \frac{\Delta C}{\Delta t} \quad (112).$$

Then, if one lets $D = l\,u$, $\Delta x = 2l$, and $\Delta C/\Delta t = \partial C/\partial t$ where l is the mixing cell length, equation (112) can be rearranged to give

$$C_{N-1} - C_N = \frac{2l}{u} \frac{dC}{dt} \tag{113}$$

where

$$N = X/2l.$$

Equation (113) is the same as equation (100) for the Nth mixing cell with the mean residence time equal to 2l/u.

The finite difference approximation to equation (111) requires that the increment ΔX be much less than the total length of the bed. Hence, this comparison is valid only for large N.

Physically it seems realistic to use the mixing cell model for high flows, but for low flows it is not realistic to assume perfect mixing in each cell. For this reason one should use either the diffusion or the random-walk model when the flow rate is small.

The random-walk and diffusion models are compared by defining

$$D = u\ l \tag{114}$$

and

$$P_e = \frac{dp}{l} = \frac{dpu}{D} \tag{115}.$$

Then it is consistent to write

$$N = \frac{L}{l} = \frac{L\,u}{D} \tag{116}.$$

A further comparison of the diffusion and the random-walk model is made by comparing the C/C_o versus θ curves of each model for a step function input. This comparison for N = 2 and N = 80 is shown in Figure 4. It is seen here that the shape and values of

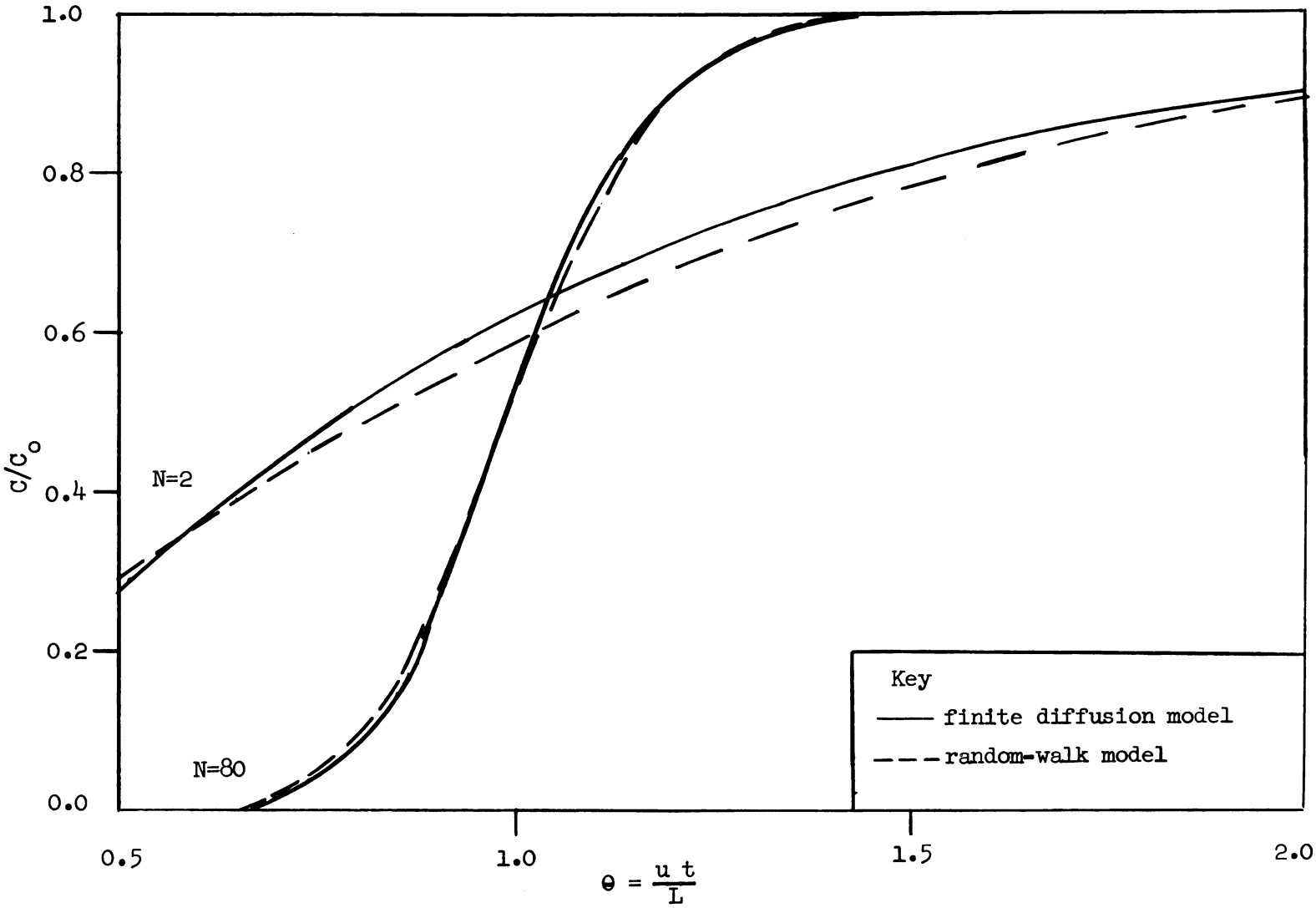

Figure 4. Comparison of the Concentration Profiles of the Diffusion and Random-Walk Models.

the curve for each model are approximately the same.

Since neither the diffusion model nor the random-walk model is completely rigorous, it makes no difference which model is used to correlate experimental data. The only criterion for choosing one model over the other is the simplicity of the calculations.

THE EXPERIMENTAL PROGRAM

It has been shown that the total spread number, ψ, of a pulse input as it passes through a column packed with an adsorbing material, is the sum of the spreads due to axial dispersion and adsorption. It is seen in equation (51) that the adsorption spread is a function of the velocity, the void fraction, the mass transfer coefficient, the equilibrium constant, and the distance between the measuring points.

If this part of the process is scaled-up such that the length, void fraction, and the velocity are unchanged; then for an increase in the column cross sectional area there is no reason to expect a change in the mass transfer coefficient or the equilibrium constant. Therefore, it is expected that the spread of the pulse due to adsorption would not be a function of the column diameter. Thus, if the total spread of a pulse is a function of the column diameter this effect is a result of axial dispersion and not adsorption. Therefore, an experimental investigation of flow in a non-adsorbing packed bed was made in order to establish the effect of column diameter on the spread of pulse input.

At the present time, it is not possible to predict a variation of the axial dispersion coefficient with column diameter. Axial dispersion has been shown to be a result of radial velocity gradients for laminar flow in a tube while for turbulent flow the dispersion results from eddy's or fluctuations. Since flow in a packed bed exhibits characteristics of both laminar and turbulent flow, it is expected that dispersion is caused by both the radial velocity gradients and fluctuations.

It is not known if these fluctuations and gradients change with the column cross section; therefore, it is necessary to determine experimentally the relationship between the axial dispersion coefficient and column diameter of a packed bed.

Viscous Fingering[11,18]. In chromatography applications it is common for the pulse of material to be separated to have a viscosity much higher than that of the solvent. It may be possible that this factor may have an over-all effect of changing the axial dispersion coefficient with a change in column cross section. This effect may be explained by the phenomenon known as viscous fingering.

Viscous fingering is a result of a difference in viscosity between the pulse of material injected and the continuous solvent phase. When a fluid of low viscosity is used to displace one of high viscosity in a packed bed, small irregularities in the velocity profile tend to become magnified. As a result "fingers" of the low viscosity fluid extend into the viscous phase, and grow exponentially with time.

For a high viscosity material displacing one of low viscosity the boundary is stable, fingers do not form. No studies have been made, however, on a pulse with a different viscosity than that of the solvent, to determine the effect on the dispersion. A pulse of high viscosity material might be expected to have a stable front boundary and an unstable rear boundary. On the other hand, it is reasonable to expect the combination of the two boundaries of a pulse to be stable. This problem is investigated in this work.

End Effects. End effects are a result of conditions at the ends of the column which disrupt the flow pattern. This disturbance in flow pattern may increase with the column cross section, possibly making the axial dispersion coefficient a function of diameter.

Objectives. The experimental objectives of this research were to determine; (a) the effect of column diameter and (b) the effect of a high viscosity pulse on dispersion in a packed bed.

In order to fulfill these objectives, it was decided to use the pulse tracer input method with two points of measurement for the determination of the axial dispersion coefficient.

The two major advantages of this method are that this input is similar to that used in chromatographic separations and requires only that the pulse be "hump like". In order to eliminate complicating adsorption effects a non-adsorbing packing was used.

Values of the axial dispersion coefficient for a pulse viscosity equal to that of the solvent were obtained in a six inch column and a one-half inch diameter column with the same packing material of two sizes over a wide flow rate range. Particular attention was given to low flow rates where data are scarce. Additional data were obtained in the six-inch column with a pulse of higher viscosity than the viscosity of the solvent.

APPARATUS AND PROCEDURE

A schematic diagram of the flow system used in the measurement of tracer concentration versus time in a non-adsorbing packed bed is shown in Figure 5. A one-half inch and a six inch diameter column were used with distances between the measuring points of six, twelve, and eighteen inches.

The Flow System. Each column consisted of various lengths of flanged pyrex pipe. The water and tracer tanks were connected to the column with one quarter inch copper tubing. The tracer and water containers were plastic lined galvanized steel pressure tanks. Nitrogen was used to drive the fluid from the tanks through the column. The outlet line had a micrometer valve for fine adjustment of the flow rate.

The Tracer. It was decided to use a dilute aqueous sodium chloride solution as a tracer. Sodium chloride concentrations are easily measured by electrolytic conductance and the properties of the system are well known.

The concentration of the sodium chloride in water was 0.5 g/l, approximately 500 parts per million. It is shown in Figure 6 that the specific conductance of sodium chloride is proportional to its concentration in the range of 0 to 700 parts per million. The value of the molecular diffusivity D_v at 30 ^{o}C is 1.84 $cm^2/sec \times 10^{-5}$ at 0.5 mol/liter concentration[24].

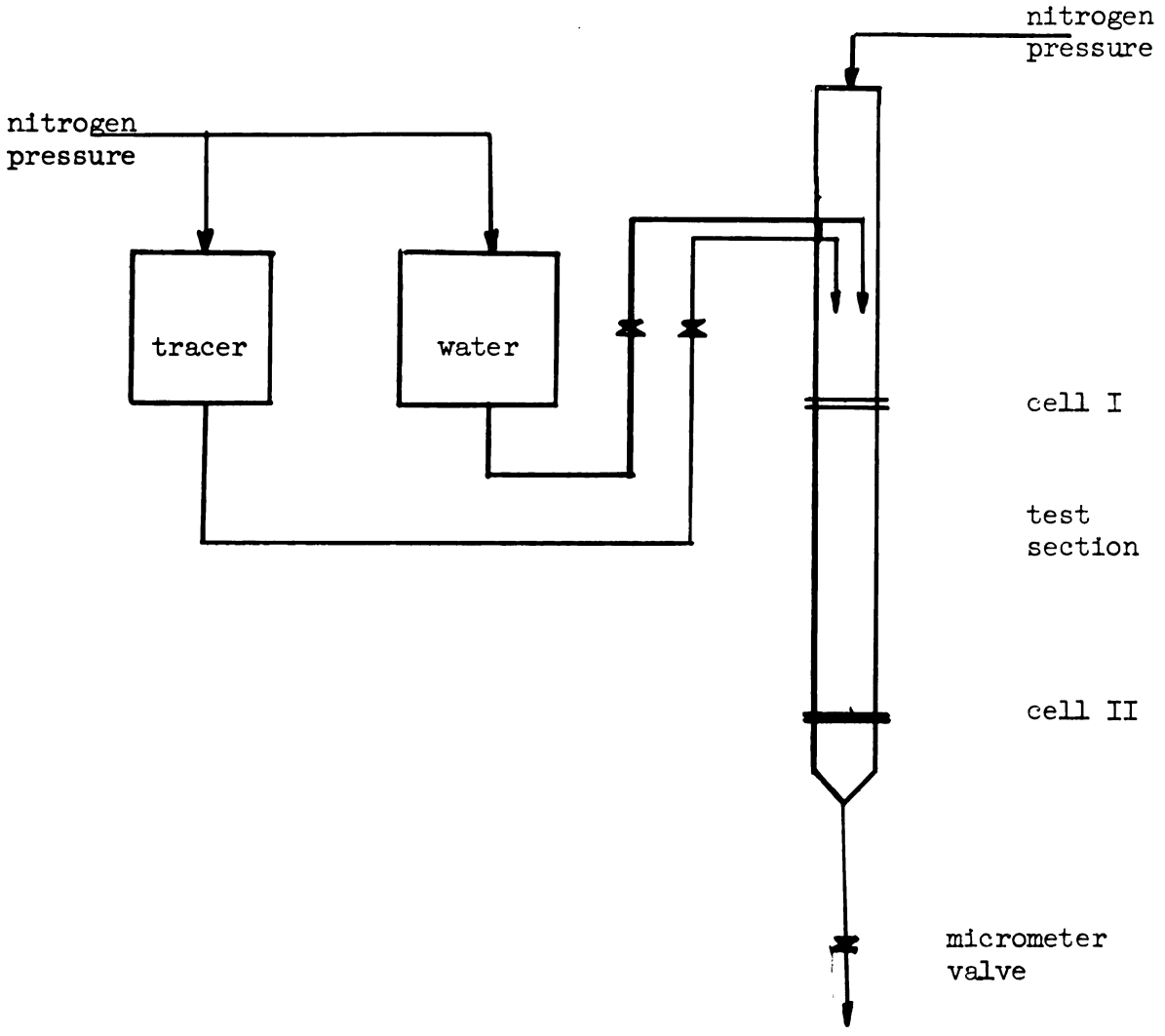

Figure 5. Schematic of Flow Equipment.

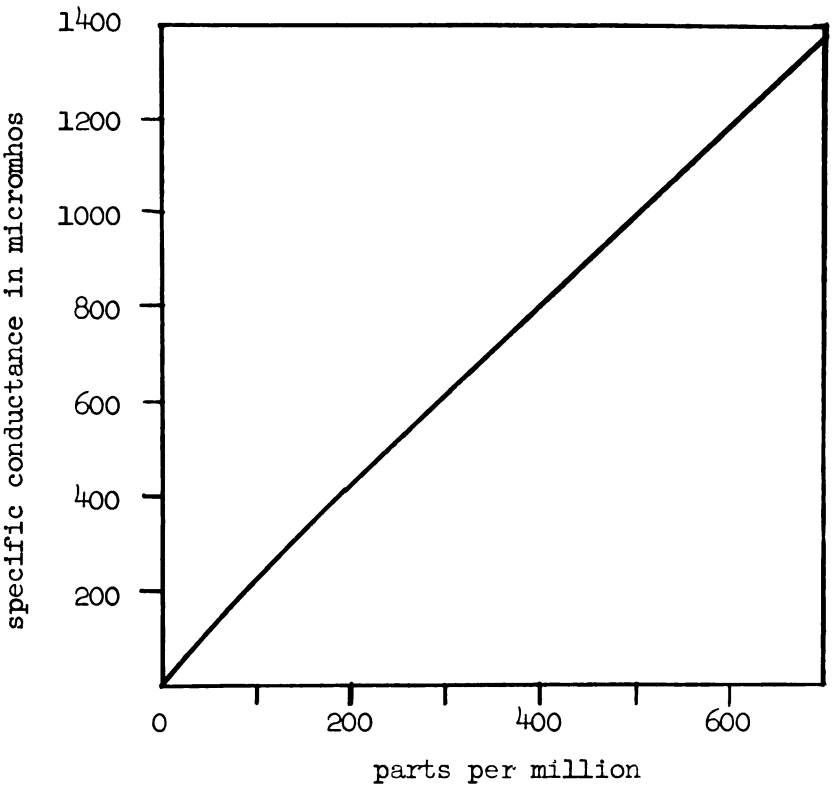

Figure 6. Specific Conductance of Sodium Chloride at 25° C.

A 65% sucrose in water with 0.035% sodium chloride was used as a tracer for the high viscosity pulse data. At room temperature this solution had a viscosity of 100 C.P. Experimental data of conductance of the sugar-NaCl solution were obtained in the laboratory since they were not available in the literature. This data is shown in Figure 7.

Packing Material. Spherically shaped glass beads of 0.0071 and 0.0047 inches were used as the packing material for this investigation.

It was experimentally verified that these beads did not adsorb sodium chloride. The conductivity of the sodium chloride solution remained unchanged after being contacted with the glass beads.

The average void fraction of these beads of 0.4 was determined by the displacement of water.

Conductance Cells. The conductivity cells for the one-half inch and the six inch columns are shown on Figures 8 and 9, respectively.

Considerable difficulty was encountered in the design and construction of reliable cells. From the standpoint of true measurements of concentration at a cross sectional plane in the bed, it would be desirable to have a sensing device which would be a part of the packed bed, or at least not change the characteristics of the bed in the region of the measuring element. Preliminary studies of various conductivity cell designs were carried out in a one inch column. Cells similar to the one shown in Figure 9 were tested in the packed bed, the cell being inserted in the packing material itself. Data on this arrangement were not reproduceable and the design was abandoned.

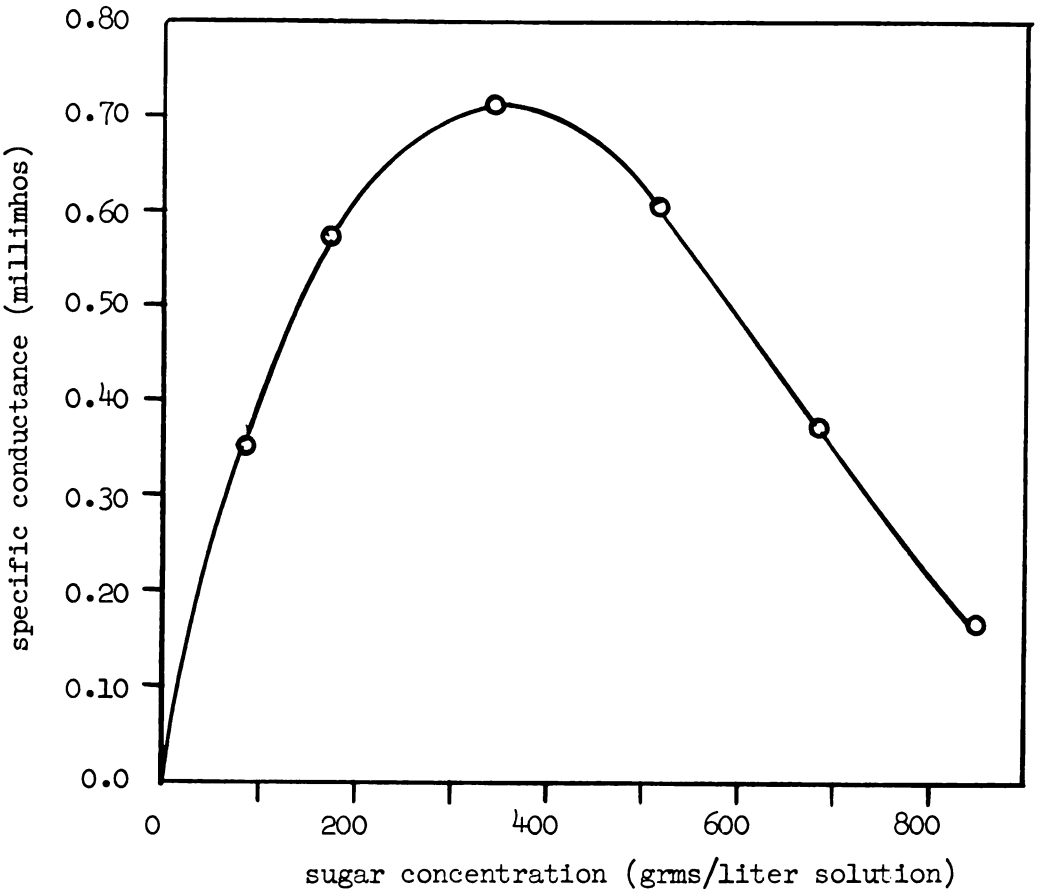

Figure 7. Specific Conductance of Sucrose with a Trace Amount of NaCl at 25° C.

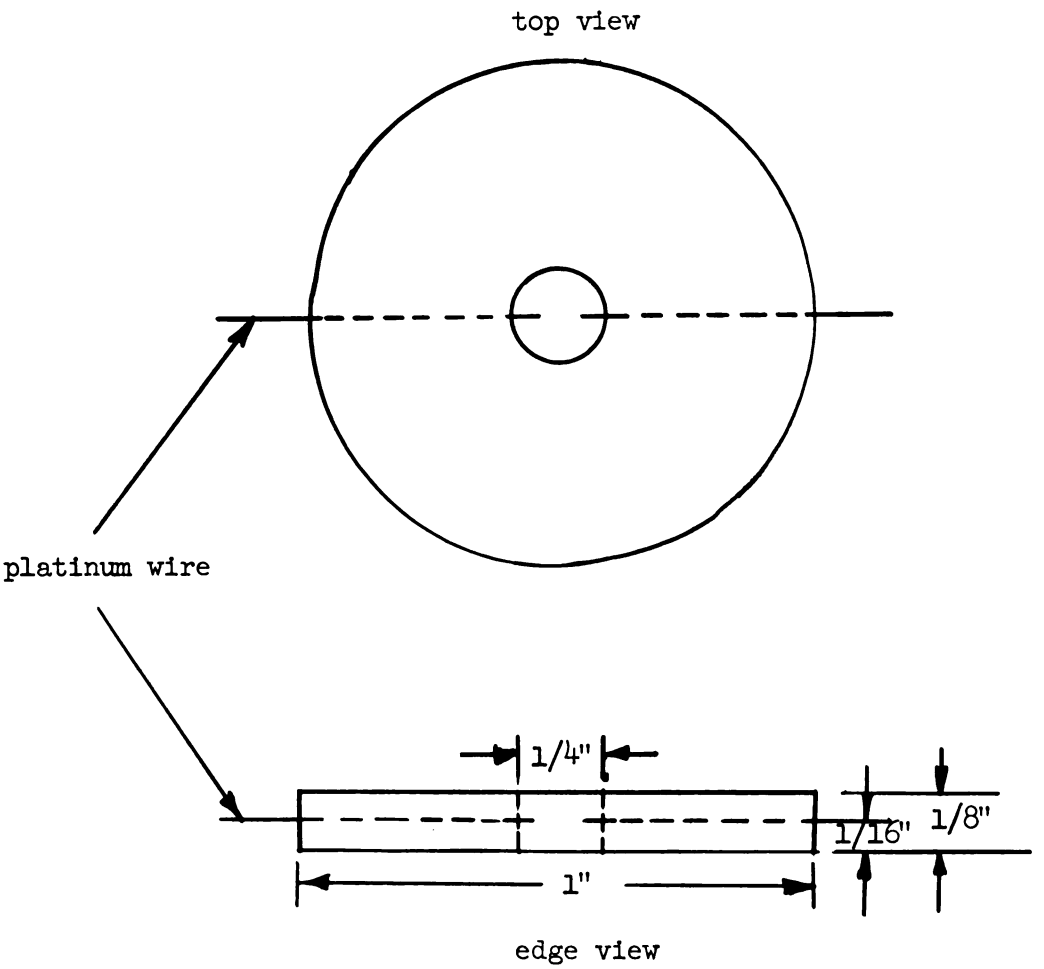

Figure 8. Plexiglas Conductivity Cell for One-half Inch Column.

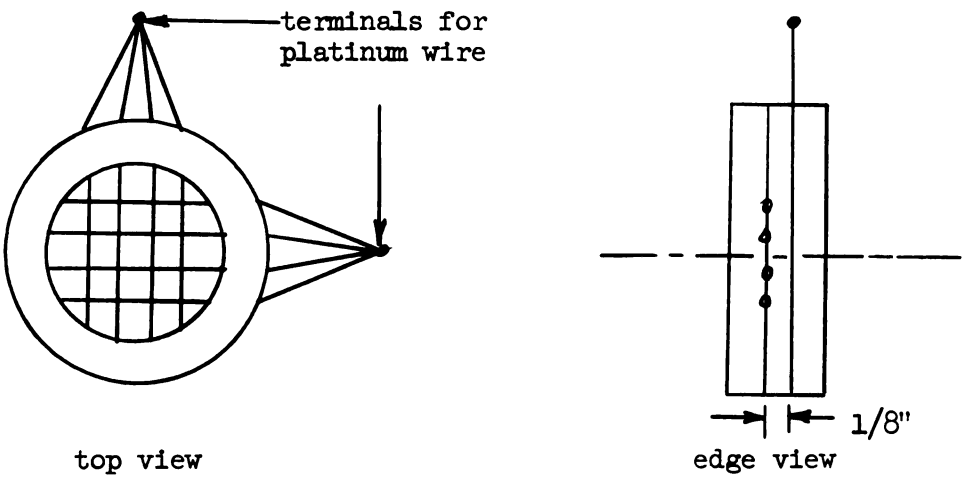

Figure 9. Six-inch Conductivity Cell.

It was then decided that the conductance cell had to be separated from the packed bed. After several other designs had been tested, the one shown in Figure 8 was tried and found to be reliable. It was inserted in the column with a piece of canvas over it to keep the packing out of the sensing area. The cell was made as thin as possible so its contribution to dispersion would be small. The amount of dispersion with this design was undetectable in the one-half inch column.

However, a similar design for the six inch column proved to be unsatisfactory, in that it contributed the equivalent of fourteen inches of packed bed to the dispersion coefficient. The improved design, shown in Figure 9, made this effect negligible.

The Measuring Circuit. The electrical circuit for measuring and recording concentration as a function of time is shown in Figure 10. The circuit is designed so that the voltage drop across the resistor R is proportional to the reciprocal of the cell resistance R_c.

The voltage drop across R is $E = IR$

where $$I = \frac{V}{R_c + R} .$$

As long as R_c is much greater than R, then

$$E = \frac{V R}{R_c}$$

Since both V and R are constant, then E is proportional to $1/R_c$ for $R_c >> R$.

R is fixed a 1 ohm and R_c is never lower than 1000 ohms. Therefore the maximum error due to this approximation is 0.1%.

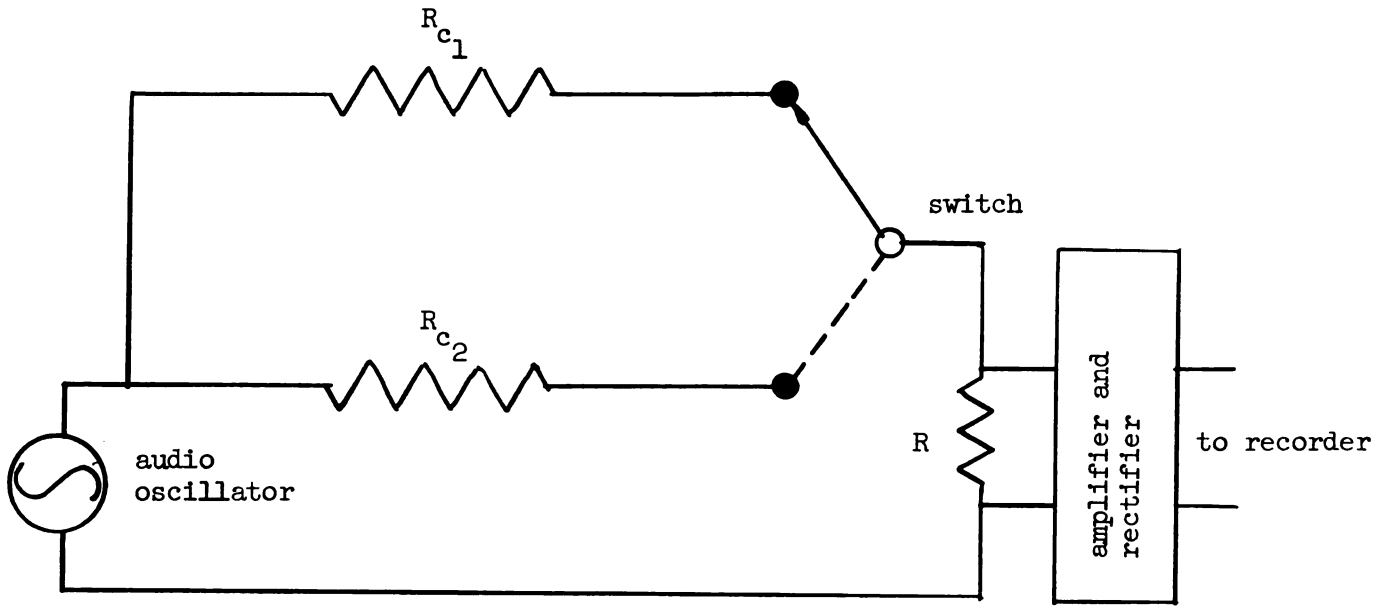

Figure 10. Electrical Circuit for Conductance Measurements.

A variable frequency audio oscillator was used as the voltage source. The A.C. voltage across R was amplified, rectified, and measured with a Sargent multi-range recorder.

A schematic diagram of the rectifying-amplifying circuit is shown in Figure 11.

Packing Procedure. It was important that considerable care be taken in packing the columns. Trapped air or unpacked channels would cause the column to operate ineffectively.

The bottom section of the column containing the packing support was filled with water. The beads were mixed as a thin slurry to remove the air from their surface and were poured into this section until it was full. During this time the column was vibrated to settle the packing.

A conductivity cell was clamped between the top of the packed section and the bottom of the next. A packing support was placed on top of the conductance cell and the packing procedure was repeated for a new section.

The column was packed to three inches above the top conductance cell and a liquid distributor with approximately the same void fraction as the packing was placed on top of the bed.

Run Procedure. While water was flowing through the bed each cell was monitored until a constant zero reading was obtained. The liquid level was allowed to drop to the top of the bed at which time the flow was stopped. A pulse of tracer was injected uniformly across

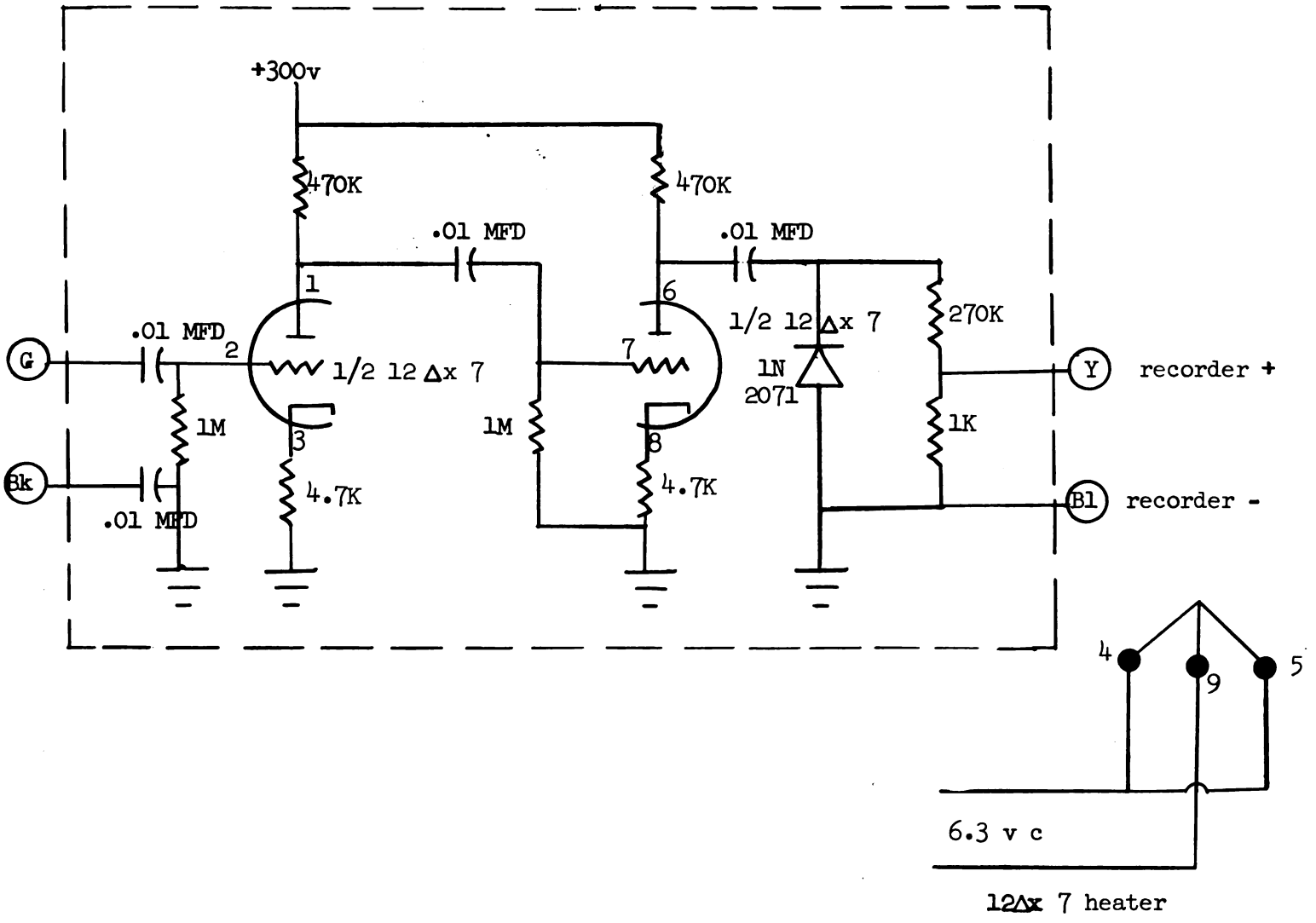

Figure 11. Schematic of Rectifying Amplifying Circuit.

the top of the bed and the flow rate was gently adjusted to allow the pulse to enter the bed, after which the water flow was resumed at the desired rate.

Conductance versus time data was obtained at each cell position in the bed.

After each run resistance versus recorder scale readings were obtained to insure that the conductance was proportional to the scale reading.

Calculation of the Dispersion Coefficient from the Data. The dispersion coefficient D is determined by the relationship

$$\frac{\sigma_2^2 - \sigma_1^2}{(\mu_2 - \mu_1)^2} = \frac{2D}{uL} \tag{50}$$

and the 2 represents cell number 2 down stream from cell number 1 where

$$\mu_n = \int_0^\infty C\, t\, \partial t \Big/ \int_0^\infty C\, \partial t \tag{27}$$

and

$$\sigma_n^2 = \int_0^\infty C\, (t - \mu_n)^2\, \partial t \Big/ \int_0^\infty C\, \partial t \tag{31}.$$

These integrals are evaluated numerically with a Control Data Corporation 3600 computer from the experimental data using Simpson's rule. Scale readings are obtained from the recorder chart at equally spaced time intervals. For the aqueous sodium chloride tracer the zero reading is subtracted from each point, these differences being

proportional to the concentration. Therefore, in place of C, in equations (27) and (31), it is necessary to insert only the corrected scale readings since the proportionality constant cancels.

For the sucrose sodium chloride tracer, the scale readings are corrected by subtracting the zero reading from each value and then obtaining the values of the concentration from Figure 7.

It can be easily verified that σ_n^2 is independent of the chosen reference time. Thus, for computational purposes, the time is taken as zero at the beginning of each cell. The time between the beginning of the two cells is noted and is added to μ_2 for the final calculation in equation (50).

The value of the interstitial velocity u is calculated from the data according to the relationship

$$U = \frac{L}{\mu_2 - \mu_1} \qquad (117).$$

Figure 12 is a plot of the conductance versus time measurements made at two positions in the column.

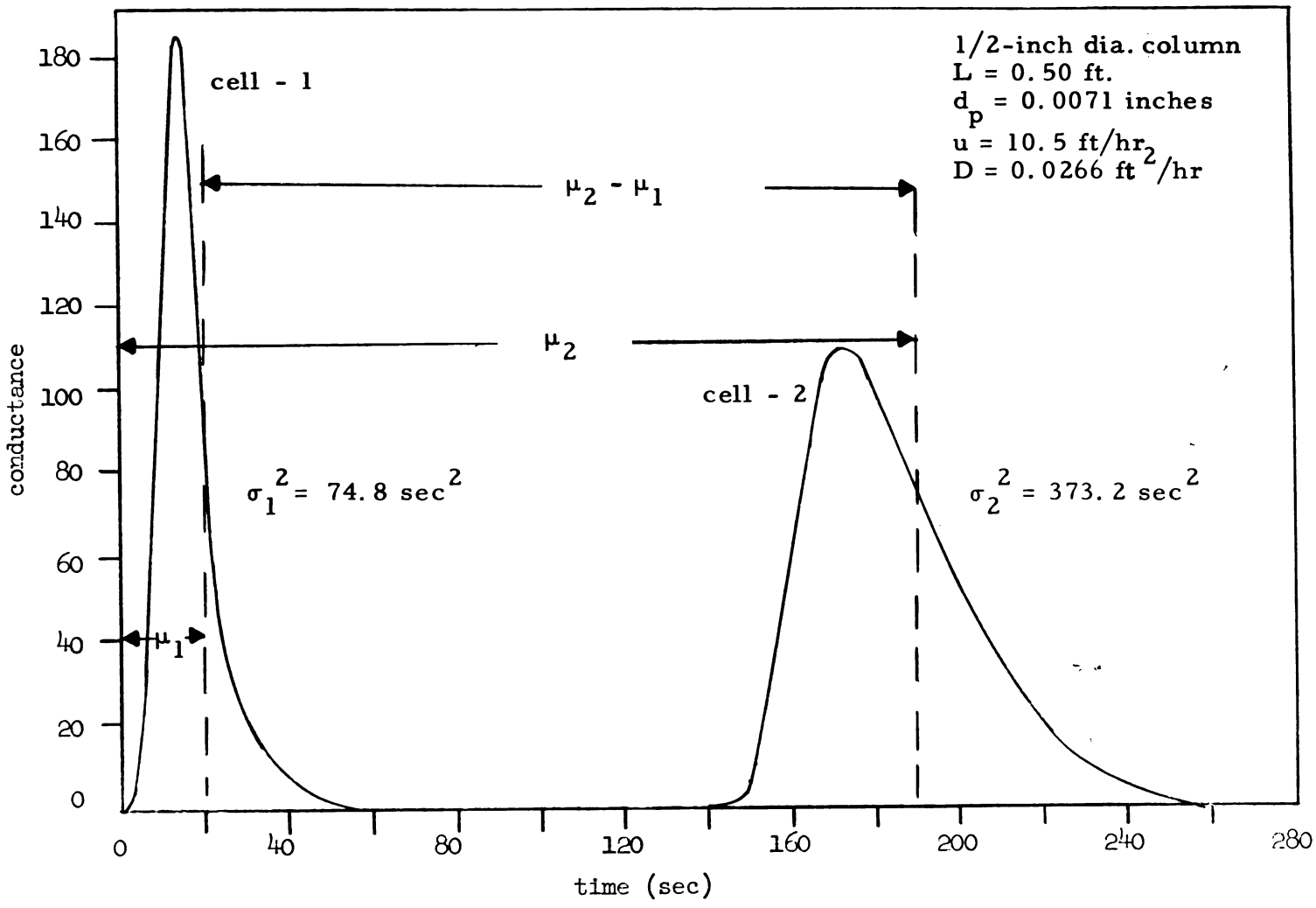

Figure 12. Conductance versus Time Plot for a Run.

RESULTS AND DISCUSSION

It is seen from equation (60)

$$D = 3.7\, d_t\, u \sqrt{\gamma} \tag{60}$$

the relationship for the eddy diffusivity for turbulent flow in a pipe, and equation (62)

$$D = d_t^2\, u^2 / 192\, D_v \tag{62}$$

the relationship for the axial dispersion coefficient for laminar flow in a pipe, that a log-log plot of D/D_v versus $d_t u/D_v$ should be a straight line. In the turbulent region the line should have a slope of 1 and in the laminar region the slope should be 2. It is expected, therefore, that the same type of plot would correlate data for packed beds, although, a straight line would not necessarily result since it may be difficult to determine the transition between turbulent and laminar flow in a packed bed. For correlation purposes, the tube diameter d_t is replaced by four times the hydraulic radius, $4M$. For a bed packed with spheres,

$$4M = \frac{2}{3} \frac{\epsilon}{1-\epsilon} d_p \ .$$

The dispersion coefficient is divided by the molecular diffusivity to illustrate that the axial dispersion coefficient should approach the magnitude of the molecular diffusivity at a low value of the velocity.

It has been pointed out that the axial dispersion coefficient should go to approximately $2/3\ D_v$ and not D_v, because the path for

the solute to diffuse is actually longer than the length of the packed bed[11].

A plot of D/D_v versus $4\ Mu/D_v$ is shown on Figure 13 for the data of this work.

Column Diameter. The effect of the column diameter was studied experimentally with six inch and one-half inch columns. It is seen from Figure 13 that there is no detectable effect of column diameter on the axial dispersion coefficient.

This data covers a range of velocities from 0.1 ft/hr to 20 ft/hr in a packed bed of spheres with a void fraction of 0.4.

Pulse Viscosity. 100 ml of 100 centipoise sugar solutions with a small amount of sodium chloride was used as a tracer. Values of the dispersion coefficient with this pulse input were obtained in the six-inch column packed with 0.0071 inch glass beads and a void fraction of 0.4. These values are compared in Figure 14 with those values obtained for an aqueous sodium chloride tracer solution where the viscosity of the pulse was the same as that of the solvent.

From this figure it can be concluded that there is no detectable effect of viscous fingering with column diameter since the values of the dispersion coefficient for a high viscosity pulse fall on the same line as those for pulse viscosity equal to that of water.

Particle Diameter. The effect of the particle diameter was studied in the one-half inch column and it is seen from Figure 15 that the dispersion coefficient effect increases with the particle diameter.

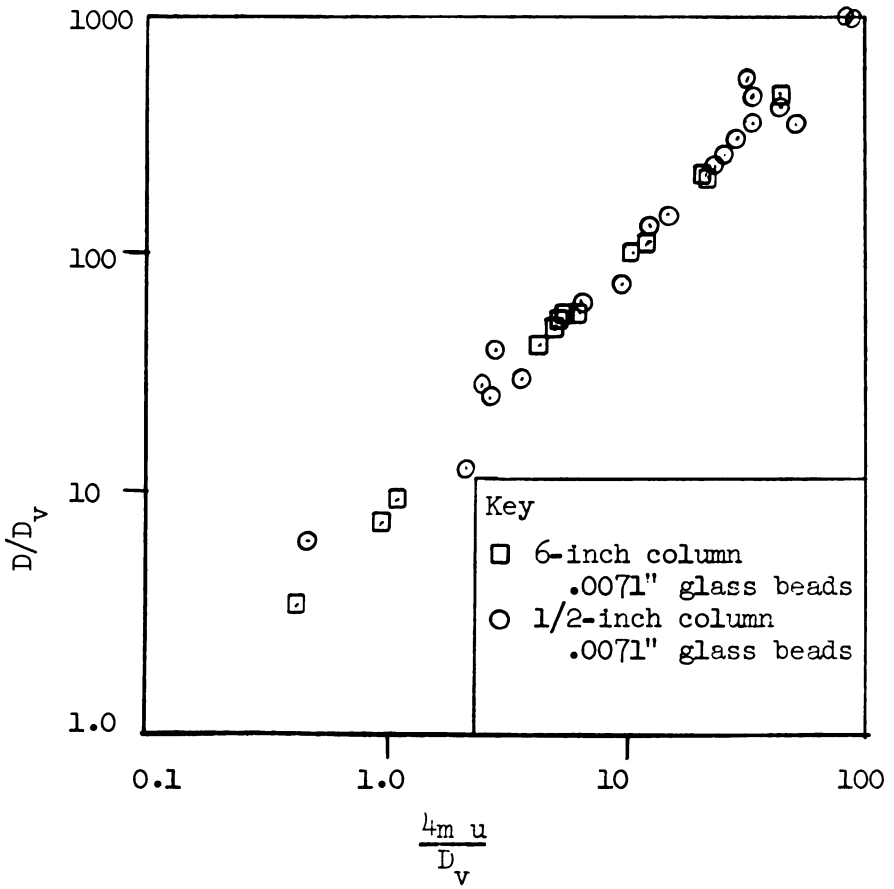

Figure 13. D/D_v versus $4Mu/D_v$ for Column Diameter Comparison.

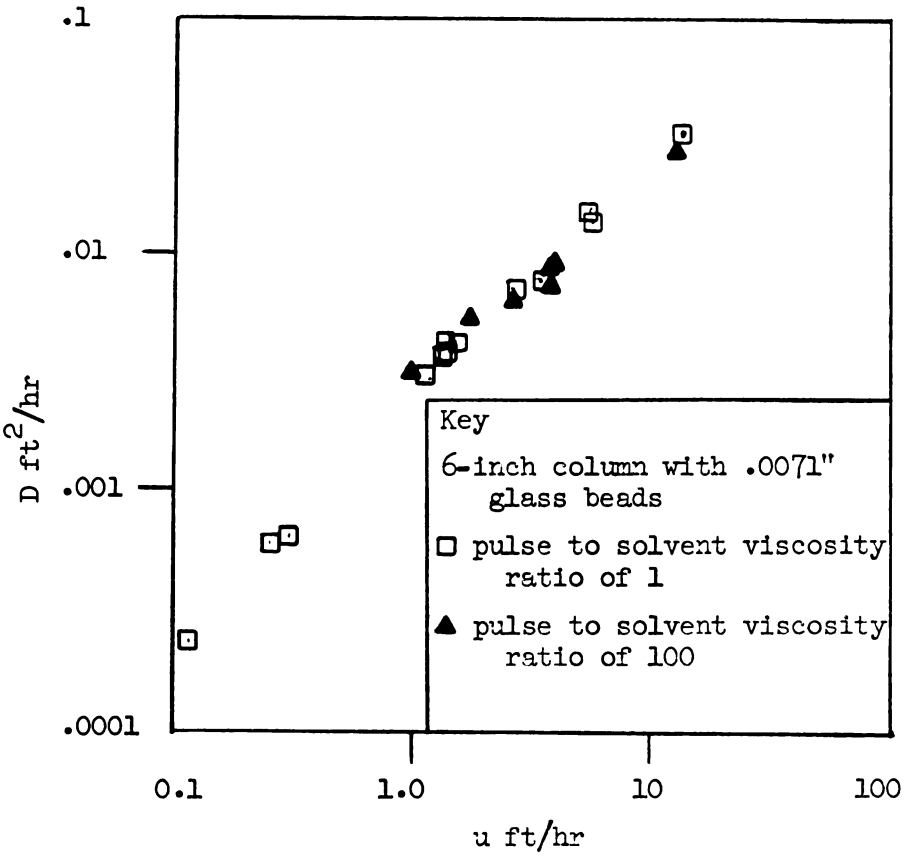

Figure 14. D versus u for Pulse Viscosity Comparison.

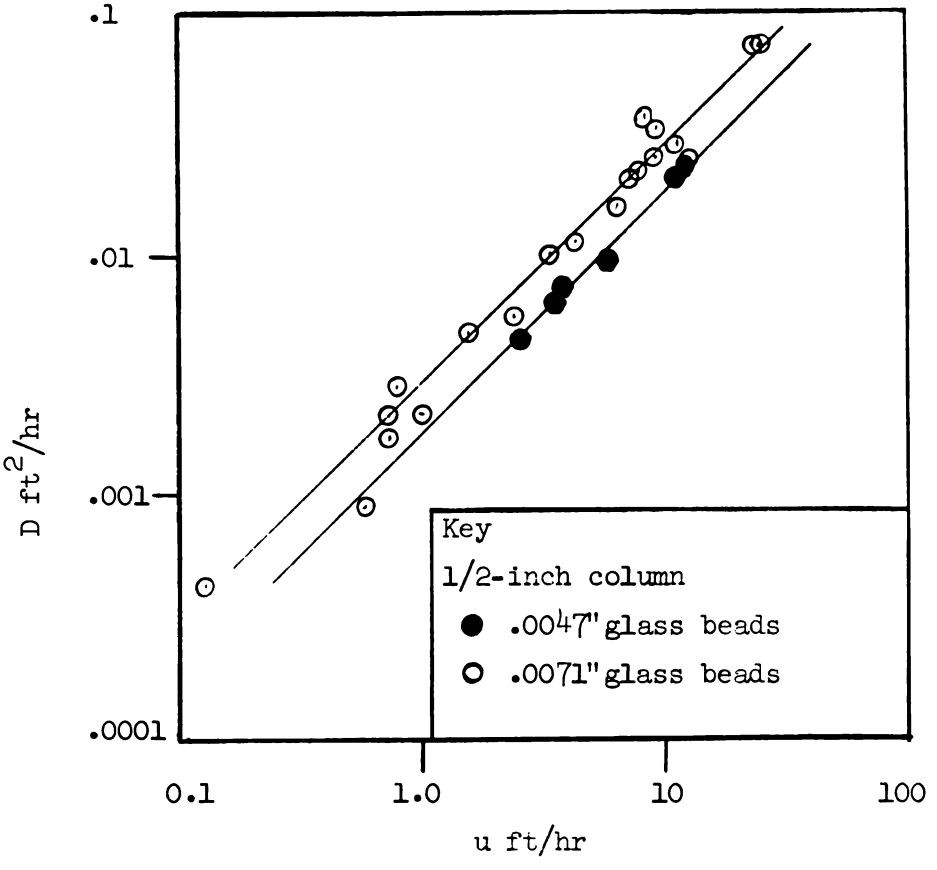

Figure 15. D versus u for Particle Diameter Comparison.

The fact that D is proportional to d_p is apparent from the correlation of Figure 16. This conclusion is in agreement with the data of Ebach and White[20] in their experimental range of $\frac{4 Mu\rho}{\mu}$ from 0.1 to 40.

Column Length. Previous investigations[16,20,38] have shown experimentally that the axial dispersion coefficient is independent of the bed length. The data obtained in both the six inch and the one-half inch columns verify their conclusion for my investigation. Values of the dispersion coefficient for these lengths are listed in Tables I through VI in Appendix IV. These values are shown on Figure 13 from which it is seen that there is no effect on the dispersion coefficient with column length.

Comparison with Other Work. Figure 17 is a plot of the packed bed Peclet Number ($P_e = \frac{ud_p}{D}$) versus a modified Reynolds Number ($Re = \frac{4 Mu\rho}{\mu}$) shows a transition range for Re between 10 and 1000. This region corresponds to the transition range between laminar and turbulent flow as illustrated by Ergun's plot[7] of the friction factor versus the Reynolds Number for packed beds.

The upper limit of the curve is described by a P_e of about 2.0 which is in excellent agreement with that predicted by the side-stepping model developed by Prausnitz[37] and, with gas phase dispersion data[35].

The lower limit of P_e is 0.22 for liquids in the experimental range. As suggested earlier, as the velocity approaches zero the axial dispersion coefficient should approach the magnitude of the

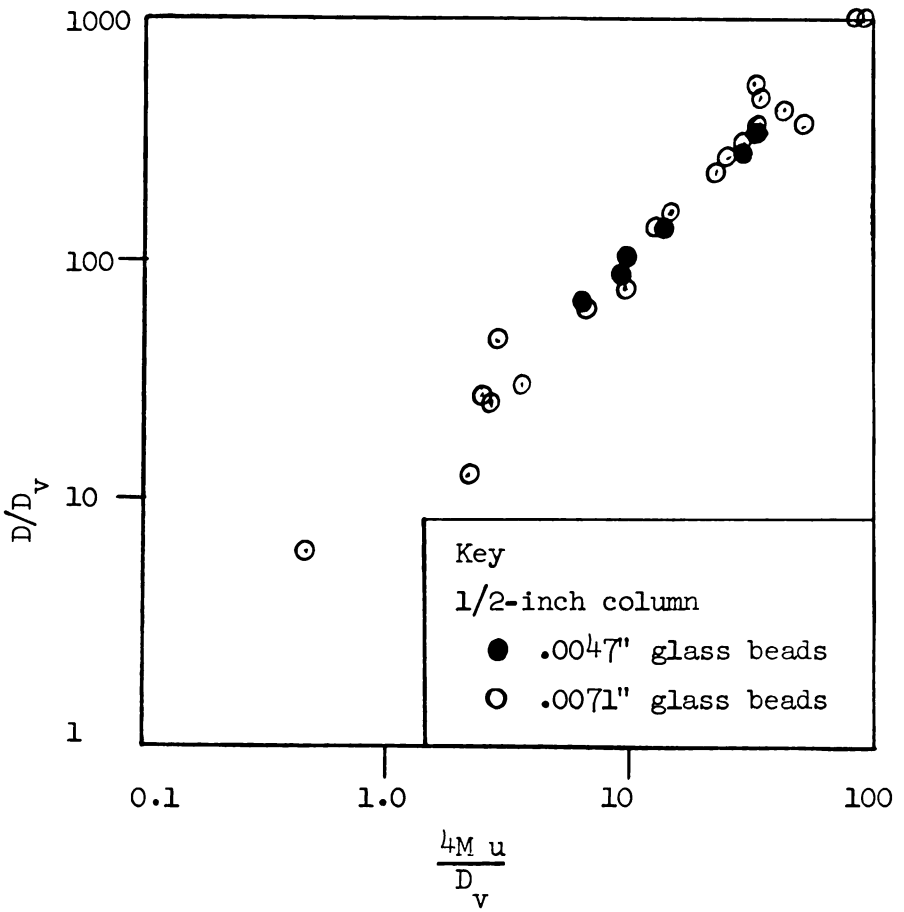

Figure 16. D/D_v versus $4Mu/D_v$ for Particle Diameter Comparison.

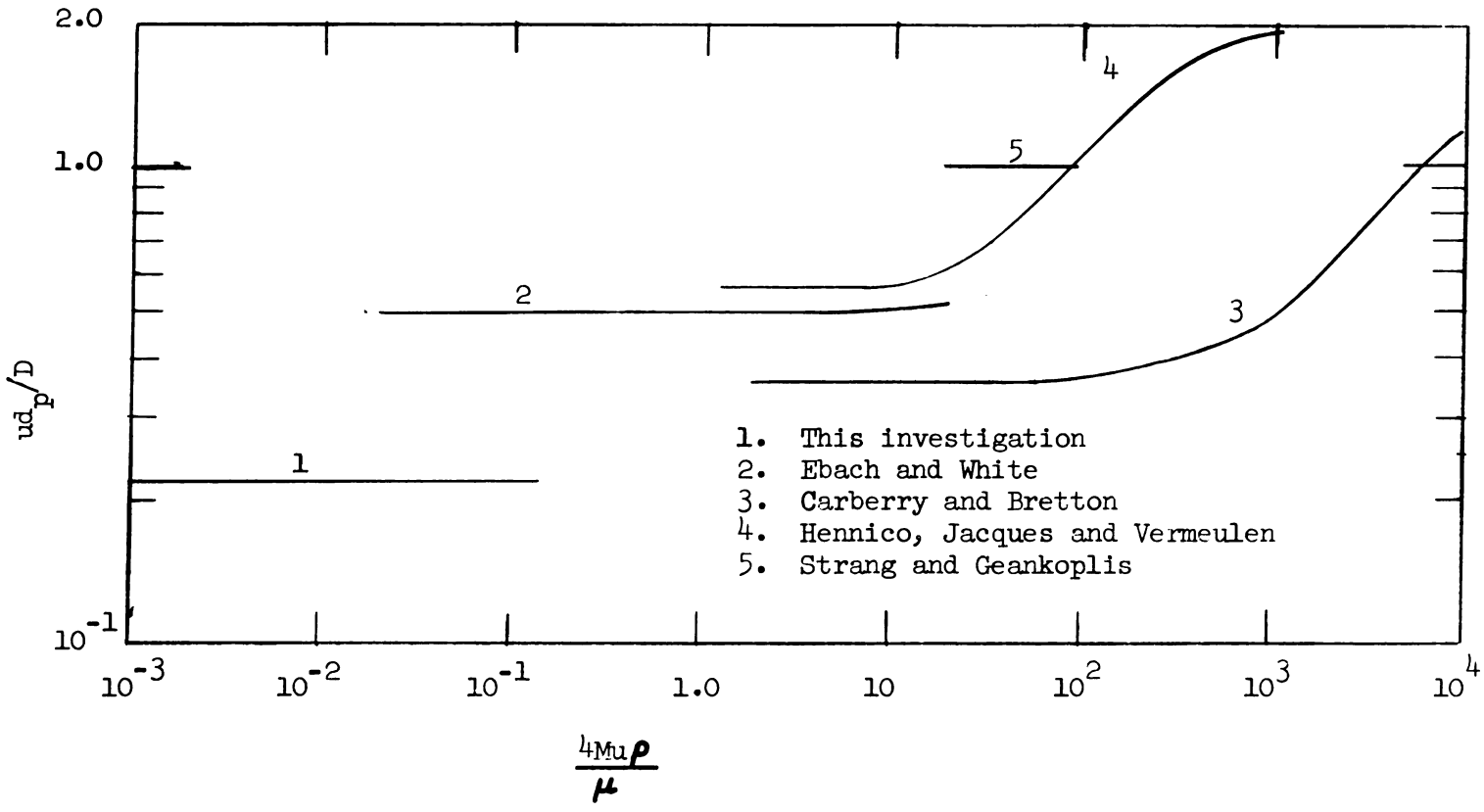

Figure 17. ud_p/D versus $4\,Mu\,\rho/\mu$ for Comparison with Other Work.

molecular diffusivity. The data obtained in this investigation at Re of 10^{-3} is in the order of magnitude of the molecular diffusivity. Consequently, one would expect P_e to go to zero with the velocity for Re less than 10^{-3}.

Ebach and White[20] used both a sinusoidal and a pulse injection of a dye into a 2.0 inch diameter column 5 feet high, packed with spheres of 0.0083, 0.04, 0.13 inches in diameter. They showed that the axial dispersion coefficient varied in proportion to the particle diameter.

Carberry and Bretton[16] used a pulse of dye into a 1.5 inch diameter column at various lengths, packed with spheres ranging from 0.02 to 0.2 inches in diameter.

Hennico, Jacques, and Vermeulen[23] used the step injection technique for spheres of 0.75 inches and 0.38 inches in diameter. They used a column diameter of 6 inches and lengths of 12 and 24 inches.

Strang and Geankopolis[41] used a sinusoidal input of dye, for 0.23 inch glass spheres in a 1.65 inch diameter and 23 inch length column.

In order to compare these experiments, one must keep many sources of error in mind, such as instrument lags, injection effects, column wall effects, and adsorption of the tracer on the particle surface. It is quite possible that the correct plotting coordinates have not been found.

In this study, the injection problem was eliminated by the use of two measuring positions. A tracer was chosen such that it

did not adsorb on the glass spheres. Since the axial dispersion coefficient was independent of column diameter, there were probably no wall effects.

CONCLUSIONS

The spread of a pulse input, as it travels through an adsorbing section of a packed bed as in chromatography, is the sum of the spreads due to axial dispersion and to adsorption. The two restrictions on this are that the input be "hump-like", and that the mass transfer process be described by a mass transfer coefficient.

There is no effect of column diameter on the axial dispersion coefficient in the range of $4mu/D_v$ from 0.5 to 80. In this range, the axial dispersion coefficient is proportional to the particle diameter. The results of this investigation are described by a constant modified Peclet Number ($P_e = 0.22$). The particle diameter effect substantiates the findings of Ebach and White[20].

The ratio of the viscosity of the pulse to that of the solvent can be as high as 100 and not affect the axial dispersion coefficient in a six inch column. It is concluded that viscous fingering has no effect on the dispersion coefficient for column diameters up to six inches, and for flow velocities within the range of 0.1 to 10 ft/hr.

The column length for short columns has no effect on the axial dispersion coefficient. This is a prime requirement for using the dispersion model, and has been verified by other investigators[16,20,38] for long columns. The dispersion coefficient is independent of column length for short beds as used in this investigation, because the experimental technique of two measuring points removed the criterion that the pulse was required to fit a normal curve as is the case for one measuring point.

APPENDIX I

The Reynolds Method of Treating Turbulence or Eddies[7].

Consider the case of one dimensional fluid flow through a packed bed. The equation of continuity of species A is:

$$D_v \frac{\partial^2 C_A}{\partial X^2} - \frac{\partial (u C_A)}{\partial X} = \frac{\partial C_A}{\partial t} \qquad (I-1)$$

In turbulent motion C_A and u are rapidly oscillating functions of time. Let a bar over a quantity represent its average value. The concentration at any time is given by:

$$C_A = \overline{C}_A + C'_A \qquad (I-2)$$

where C'_A is a time dependent concentration fluctuation.

Thus,

$$\overline{C}'_A = 0$$

Similarly,

$$u = \overline{u} + u' \qquad (I-3)$$

and

$$\overline{u}' = 0$$

where

u = the velocity

$\overline{u}$ = time average velocity

u' = velocity fluctuation.

Inserting the values for C_A and u into equation (I-1), one obtains:

$$D_v \frac{\partial^2(\overline{C}_A+C'_A)}{\partial X^2} - \frac{\partial [(\overline{C}_A+C'_A)(\overline{u}+u')]}{\partial X} = \frac{\partial(\overline{C}_A+C'_A)}{\partial t} \qquad (I-4)$$

By time averaging this equation, one is left with:

$$D_v \frac{\partial^2 \overline{C}_A}{\partial X^2} - \frac{\partial(\overline{C}_A u)}{\partial X} - \frac{\partial(\overline{C}_A' u')}{\partial X} = \frac{\partial \overline{C}_A}{\partial t} \qquad \text{(I-5)}$$

Then, $C_A' u'$ is the turbulent flux and it can be seen by analogy with Fick's law of diffusion that:

$$J\,(\text{eddy}) = - D\,(\text{eddy}) \frac{\partial C_A}{\partial X} \qquad \text{(I-6)}$$

and

$$D\,(\text{eddy}) = - \overline{C}_A' u' / \frac{\partial \overline{C}_A}{\partial X} \qquad \text{(I-7)}$$

Thus, the equation of conservation may be rewritten with the previous analogy:

$$[D_v + D(\text{eddy})] \frac{\partial^2 \overline{C}_A}{\partial X^2} - \frac{\partial(\overline{u}\,\overline{C}_A}{\partial X} = \frac{\partial \overline{C}_A}{\partial t} \qquad \text{(I-8)}$$

and the total axial diffusivity is made up of two terms, the molecular diffusivity, and the eddy diffusivity.

APPENDIX II

Explanation of Pulse Skewness.

The solution to the differential equation[31]:

$$D \frac{\partial^2 C}{\partial Z^2} = \frac{\partial C}{\partial t} \qquad \text{(II-1)}$$

where

$$Z = X - u\,t \qquad \text{(II-2)}$$

for an infinite bed with a tracer injected instantaneously at X = 0 is:

$$\frac{CV}{Q} = \frac{\exp\left[-(1 - \frac{W}{V}t)^2\right]/4\,(\frac{W}{V}t)(\frac{D}{uL})}{2\sqrt{\pi\,(\frac{X}{V}t)\,D/uL}} \qquad \text{(II-3)}$$

where

V = the volume of the bed considered

Q = amount of tracer injected

W = volumetric flow rate of solvent

L = the value of X where curve is obtained

t = time.

Figure 18 is a plot of $\frac{CV}{Q}$ versus $\frac{W}{V}t$ for several values of D/uL.

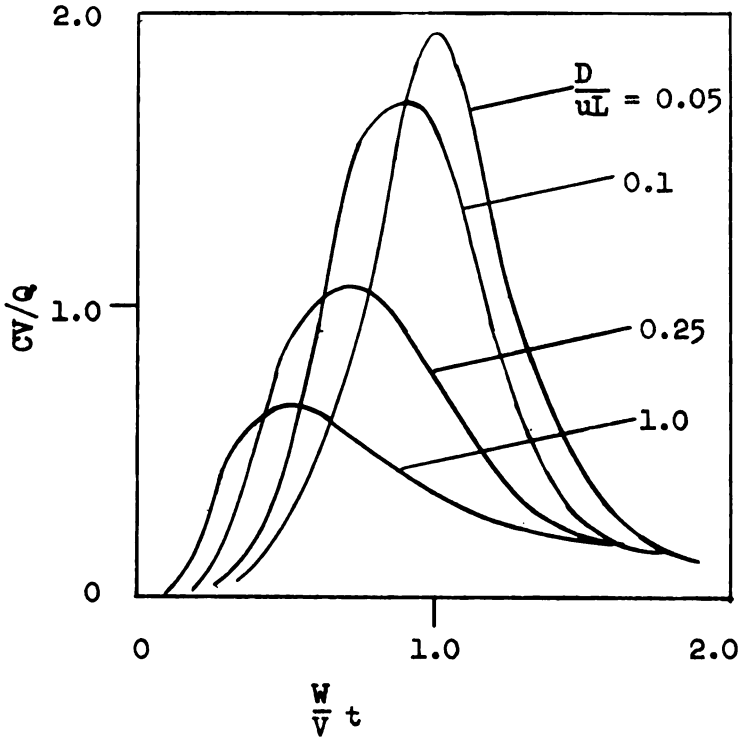

Figure 18. Plot of CV/Q versus $\frac{W}{V}$ t to Show Skewness.

The concentration approaches a Gaussian distribution for low values of D/uL, but for high values, the curves become skewed. For small values of D/uL, equation (3) can be approximated by:

$$\frac{CV}{Q} = \frac{1}{2\sqrt{\pi\, D/uL}} \exp\left[-(1-\frac{Wt}{V})^2/4D/uL\right] \qquad \text{(II-4)}$$

which is a normal distribution.

By differentiation of equation (3) with respect to t, and setting the derivative equal to zero, the time when the maximum concentration appears is

$$\frac{W}{V}\, t_m = \sqrt{(D/uL)^2 + 1} \; - \; D/uL \qquad \text{(II-5)}$$

Thus, the maximum concentration always occurs between values of $\frac{Wt}{V}$ of 0 and 1. For small values of D/uL, $\frac{Wt}{V}$ is about 1, while for larger values, it is significantly less than 1.

APPENDIX III

The solution to equation (104).

$$C_N = \frac{1}{N!} \left(\frac{W}{V}\right)^{N+1} \int_0^t C_f (t-s)^N \exp\left[- \frac{W}{V} (t-s)\right] ds \qquad (104)$$

The solution for a delta pulse function input, that is with the condition:

$$C_f = C_i \qquad 0 < t < \delta$$

$$C = 0 \qquad t < 0 \text{ and } t > \delta$$

is a tabulated integral. The solution to this equation is

$$\frac{C_N}{C_i} = \exp\left[- \frac{W}{V} (t-\delta)\right] \left[\left[\frac{W}{V} \frac{(t-\delta)}{N!}\right]^N + \frac{\left[\frac{W}{V}(t-\delta)\right]^{N-1}}{(N-1)!} + \ldots + 1 \right]$$

$$- \exp\left[- \frac{W}{V} t\right] \left[\left(\frac{W}{V} t\right)^N / N! + \ldots + 1 \right] \qquad (III-1)$$

This is the same result obtained if one superimposed two step inputs; the first step followed after time δ by a solvent step.

Equation (1) is simplified by expanding the $(t-\delta)^N$ terms according to the binomial expansion along with expanding the $\exp\left[\frac{W}{V} \delta\right]$ term, and then dropping all second and higher order terms of δ.

With this approximation, there results

$$\frac{C_N}{C_i} = \left[\left(\frac{W}{V} t\right)^{N+1} \frac{1}{N!} \right] \frac{\delta}{t} \exp\left[- \frac{W}{V} t\right] \qquad (III-2)$$

and $C_i \delta$ is replaced by Q/W and then

$$\frac{C_N V}{Q} = \left(\frac{W t}{V}\right)^N \frac{1}{N!} \exp\left[-\frac{W}{V} t\right] \qquad \text{(III-3)}$$

Table I

Data for 1/2-inch column
.0071 inch glass beads
3 cells equally spaced
12 inches long

u ft/hr	$4 Mu/D_v$	*1 ft^2/hr			*2		
		D_{1-2}	D_{2-3}	D_{1-3}	D_{av}/D_v	ud_p/D_{av}	$4 Mu\rho/\mu$
23.8	88.1	--	--	0.0720	1001.0	0.198	0.162
23.4	86.5	--	--	0.0720	1001.0	0.194	0.159
13.5	50.0	0.0257	0.0258	0.0258	362.0	0.311	0.092
10.5	38.8	0.0266	--	--	378.0	0.251	0.072
9.0	33.0	--	--	0.0265	372.0	0.200	0.061
7.95	29.4	0.0217	0.0219	0.0219	308.0	0.216	0.054
7.18	26.6	0.0210	0.0191	0.0200	281.0	0.214	0.049
6.35	23.5	0.0179	0.0169	0.0174	244.0	0.216	0.043
3.31	12.2	0.0091	0.0107	0.0103	145.0	0.189	0.022
2.56	9.5	0.0054	0.0055	0.0055	77.2	0.277	0.017
1.74	6.4	0.0046	--	--	64.5	0.223	0.012
0.795	2.94	0.0029	--	--	40.6	0.162	0.0054
0.72	2.66	0.0021	0.0021	0.0021	29.4	0.203	0.0049
0.583	2.16	0.00091	--	--	12.7	0.383	0.0040
0.131	0.485	0.000448	--	--	6.3	0.173	0.00089

*1 D_{1-2}, D_{2-3}, and D_{1-3} are calculated from the spread between the first and second, second and third, and the first and third cells, respectively.

*2 D_{av} = the average value of D_{1-2}, D_{2-3}, and D_{1-3}.

Table II

Data for 1/2-inch column
.0071 inch glass beads
2 cells 18 inches apart

u ft/hr	$4 Mu/D_v$	D ft^2/hr	D/D_v	ud_p/D	$4 Mu\rho/\mu$
9.15	33.9	0.0324	470.0	0.162	0.062
8.6	31.8	0.0379	534.0	0.135	0.058
4.15	15.4	0.0112	157.0	0.221	0.028
1.0	3.7	0.0022	30.8	0.270	0.0068
0.72	2.66	0.0018	26.1	0.230	0.0049

Table III

Data for 1/2-inch column
.0047 inch glass beads
2 cells 18 inches apart

u ft/hr	$4 Mu/D_v$	D ft^2/hr	D/D_v	ud_p/D	$4 Mu\rho/\mu$
12.8	31.4	0.0243	341.0	0.207	0.058
11.9	29.2	0.0212	298.0	0.221	0.054
5.95	14.6	0.0098	138.0	0.239	0.027
3.96	9.7	0.0075	105.0	0.207	0.018
3.80	9.3	0.0062	87.0	0.241	0.017
2.72	6.7	0.0044	61.6	0.245	0.012

Table IV

Data for 6-inch column
.0071 inch glass beads
3 cells 6 and 12 inches apart

u ft/hr	$4 Mu/D_v$	*1 ft^2/hr D_{1-2}	D_{2-3}	D_{1-3}	*2 D_{av}/D_v	ud_p/D_{av}	$4 Mu\rho/\mu$
11.40	42.2	0.0331	0.0344	0.0338	473.0	0.200	0.078
5.85	21.6	0.0149	0.0156	0.0150	212.0	0.230	0.040
5.60	20.7	0.0148	0.0158	0.0162	219.0	0.214	0.038
3.40	12.6	--	--	0.0077	108.0	0.263	0.023
2.82	10.4	0.0075	0.0069	0.0070	101.0	0.232	0.019
1.70	6.3	--	--	0.0042	59.0	0.241	0.012
1.57	5.8	0.0040	0.0038	0.0041	56.2	0.232	0.011

*1 D_{1-2}, D_{2-3}, and D_{1-3} are calculated from the spread between the first and second; second and third; and the first and third cells, respectively.

*2 D_{av} = the average value of D_{1-2}, D_{2-3}, and D_{1-3}.

Table V

Data for 6-inch column
.0071 inch glass beads
2 cells 12 inches apart

u ft/hr	$4 Mu/D_v$	D ft^2/hr	D/D_v	ud_p/D	$4 Mu\rho/\mu$
1.460	5.4	0.0040	56.2	0.216	0.0099
1.380	5.1	0.0036	50.5	0.225	0.0094
1.190	4.4	0.0030	42.2	0.234	0.0081
0.300	1.1	0.00066	9.23	0.268	0.0020
0.260	0.96	0.00061	8.55	0.252	0.0018
0.113	0.42	0.00023	3.24	0.293	0.00077

Table VI

Data for 100 Centipoise Sugar Solution with a Trace of NaCl as Pulse

6-inch column
.0071 inch glass beads
2 cells 1.5 ft apart

u ft/hr	D ft^2/hr	ud_p/D	4 Mup/μ
11.4	0.0281	0.241	0.0774
3.95	0.0096	0.243	0.0268
3.91	0.0079	0.293	0.0266
3.91	0.0091	0.254	0.0266
2.67	0.0068	0.232	0.0181
1.83	0.0054	0.200	0.0123
0.98	0.0021	0.277	0.0067

NOMENCLATURE

A	-	Cross-sectional area of tube.
a	-	Area of solids/volume.
C	-	Normalized concentration (defined by equation 10).
C_A	-	Concentration of component A mol/vol.
C_{Ai}	-	Concentration of A at the solid interface.
C_{As}	-	Concentration of A on the solid (mols/vol. solid).
D	-	Axial dispersion coefficient in adsorbing section.
D_b	-	Axial dispersion coefficient in non-adsorbing section.
D_v	-	Molecular diffusivity of solute.
d_p	-	Particle diameter.
d_t	-	Tube diameter.
L	-	Distance between measuring points.
K_x	-	Mass transfer coefficient (mols ft/time Conc. driving force).
m	-	Equilibrium constant between solid and liquid (defined by equation 5).
M	-	Hydraulic radius for packed bed
p	-	Laplace transform variable.
Q	-	Total amount of solute injected.
t	-	Time.
u	-	Interstitial velocity.
W	-	Volumetric flow rate.
x	-	Distance variable.
δ	-	Incremental time for pulse to be introduced.

ϵ - Void fraction.

ζ - Distance from second measuring point to end of adsorbing sector.

μ_m - The mean time of C-t at X_m.

μ_o - The mean time of C-t at X_o.

μ - Viscosity of solvent.

ψ - Spread of pulse (defined by equation 46).

ψ_D - Spread of pulse due to dispersion (defined by equation 47).

ψ_A - Spread of pulse due to adsorption (defined by equation 48).

ρ - Density of solvent.

σ_m^2 - The variance of C-t at X_m.

σ_o^2 - The variance of C-t at X_o.

BIBLIOGRAPHY

1. Aris, R., Chem. Eng. Sci., 11, 194 (1959).
2. Aris, R., Chem. Eng. Sci., 9, 266 (1959).
3. Aris, R., Chem. Eng. Sci., 11, 194 (1959).
4. Aris, R., Proc. Roy. Soc., A235, 67 (1956).
5. Aris, R., Proc. Roy. Soc., A245, 268 (1958).
6. Aris, R. and Amundson, N. R., A.I.Ch.E. Journal, 3, 280 (1957).
7. Bird, R. B., Stewart, W. E., and Lightfoot, E.N., Transport Phenomena, John Wiley & Sons, Inc., New York, (1960), p. 626.
8. Bischoff, K. B., and Levenspiel, O., Chem. Eng. Sci., 17, 245 (1962).
9. Bischoff, K. B., and Levenspiel, O., Chem. Eng. Sci., 17, 257 (1962).
10. Bischoff, K. B., Can. Journal Chem. Eng., 41, 129 (1963).
11. Blackwell, R. J., Rayne, J. R., and Terry, W. M., Mining Metallurgical and Petroleum Engineers, Transactions A.I. M.E., 216, 1 (1959).
12. Brenner, H., Chem. Eng. Sci., 17, 229 (1962).
13. Cairns, E. J., and Prausnitz, J. M., Ind. Eng. Chem., 51, 1441 (1959).
14. Cairns, E. J., and Prausnitz, J. M., Chem. Eng. Sci., 12, 20 (1960).
15. Carberry, J. J., A.I.Ch.E. Journal, 4, 13M (1958).
16. Carberry, J. J., and Bretton, R. H., A.I.Ch.E. Journal, 4, 367 (1958).

17. Carlslaw, H. S., and Jaeger, J. C., Conduction of Heat in Solids, 2nd ed., Oxford Press (1959), pp. 114-120, 491-2, 494-6.

18. Collins, R. E., Flow of Fluids Through Porous Materials, Reinhold Pub. Corp., New York (1961), pp. 196-200.

19. Danchkwerts, P. V., Chem. Eng. Sci., 2, 1 (1953).

20. Ebach, E. A., and White, R. R., A.I.Ch.E. Journal, 4, 161 (1958).

21. Geankopolis, G. S., and Liles, A. W., A.I.Ch.E. Journal, 6, 591 (1960).

22. Heller, J. P., A.I.Ch.E. Journal, 9, 452 (1963).

23. Hennico, A., Jacques, G., and Vermeulen, T., Longitudinal Dispersion in Packed Extraction Columns, U. of Calif., Berkeley, U. S. Atomic Energy Comm. (1963).

24. International Critical Tables, McGraw Hill Book Co., Inc., New York.

25. Jacques, G., and Vermeulen, T., Longitudinal Dispersion in Solvent Extraction Columns: Peclet Numbers for Ordered and Random Packings, University of California, Berkeley, U. S. Atomic Energy Comm. (1957).

26. Jacques, G. L. Cotter, J. E., and Vermeulen, T., Longitudinal Dispersion in Packed Extraction Columns, U. of Calif., Berkeley, U. S. Atomic Energy Comm. (1959), UCRL-8658.

27. Klinkenberg, A. R., Ind. Eng. Chem., 46, 2285 (1954).

28. Klinkenberg, A. R., Ind. Eng. Chem., 45, 1202 (1953).

29. Klinkenberg, A. R., and Sjenitzer, F., Chem. Eng. Sci., 5, 258 (1956).

30. Kramers, H., and Alberda, G., Chem. Eng. Sci., 2, 173 (1953).

31. Levenspiel, O., and Smith, W. K., Chem. Eng. Sci., 6, 227 (1957).

32. Levenspiel, O. A., Can. Journal of Chem. Eng., 41, 132 (1963).

33. Levenspiel, O., Can. Journal of Chem. Eng., 40 (1962).

34. Mirjarichi, T., and Vermeulen, T., Ind. Eng. Chem., Fundamentals, 2, 304 (1963).

35. McHenry, K. W., and Wilhelm, R. H., A.I.Ch.E. Journal, 3, 83 (1957).

36. Prausnitz, J. M., and Wilhelm, R. H., Ind. Eng. Chem., 49, 978 (1957).

37. Prausnitz, J. M., A.I.Ch.E. Journal, 4, 14M (1958).

38. Rifai, M. E., Ph.D. Dissertation, U. of Calif., Berkeley (1956).

39. Scheidegger, A. E., The Physics of Flow Through Porous Media, MacMillan Co., New York (1957).

40. Scheidegger, A. E., Journal Appl. Phys., 25, 994 (1954).

41. Strang, D. A. and Geankoplis, C. J., Ind. Eng. Chem., 50, 1305 (1958).

42. Taylor, G. I., Proc. Roy. Soc., A223, 446 (1954).

43. Taylor, G. I., Proc. Roy. Soc., A219, 186 (1953).

44. Turner, J. C. R., Ind. Eng. Chem., Fundamentals, 3, 88 (1964).

45. VanDeemter, J. J., Zuiderweg, F. J., and Klinkenberg, A. R., Chem. Eng. Sci., 5, 271 (1956).

46. Van der Laan, E., Chem. Eng. Sci., 7, 187 (1958).

47. Von Rosenberg, D. U., A.I.Ch.E. Journal, 2, 55 (1956).

48. Wehner, J. F., and Wilhelm, R. H., Chem. Eng. Sci., 6, 89 (1956).

49. White, R. R., Can. Journal Chem. Eng., 41, 131 (1963).

50. Zweitering, T. N., Chem. Eng. Sci., 11, 1 (1959).